

Risk Bounds For Distributional Regression

Carlos Misael Madrid Padilla¹ Oscar Hernan Madrid Padilla²
Sabyasachi Chatterjee³

¹Department of Statistics and Data Science, Washington University in St Louis

²Department of Statistics, University of California, Los Angeles

³Department of Statistics, University of Illinois at Urbana-Champaign

February 8, 2025

Abstract

This work examines risk bounds for nonparametric distributional regression estimators. For convex-constrained distributional regression, general upper bounds are established for the continuous ranked probability score (CRPS) and the worst-case mean squared error (MSE) across the domain. These theoretical results are applied to isotonic and trend filtering distributional regression, yielding convergence rates consistent with those for mean estimation. Furthermore, a general upper bound is derived for distributional regression under non-convex constraints, with a specific application to neural network-based estimators. Comprehensive experiments on both simulated and real data validate the theoretical contributions, demonstrating their practical effectiveness.

Keywords: Nonparametric distribution estimation, isotonic, trend filtering, dense ReLU networks.

1 Introduction

While regression methods are widely popular across statistics and machine learning, it is well recognized that the conditional mean alone often fails to capture the full relationship between a response variable and a set of covariates. A common extension is quantile regression, which estimates conditional quantiles to provide a more detailed view of the response distribution (Koenker and Bassett Jr, 1978). A more direct approach is distributional regression, which estimates the conditional distribution of the response given the covariates.

Distributional regression has found applications in diverse areas, including electricity spot price analysis (Klein, 2024), understanding income determinants (Kneib et al., 2023), modeling weather data (Umlauf and Kneib, 2018), and improving precipitation forecasts (Henzi et al., 2021; Schlosser et al., 2019).

The estimation of distributions of random variables under structural constraints is a fundamental problem in many statistical and machine learning tasks, including nonparametric regression, density estimation, and probabilistic forecasting (Hastie et al., 2009; Tibshirani, 2014; Guntuboyina et al., 2020). Given independent observations $y_1, \dots, y_n \in \mathbb{R}^n$ from unknown distributions

F_1^*, \dots, F_n^* , the objective of this paper is to estimate the vector $F^*(t) = (F_1^*(t), \dots, F_n^*(t))^\top$ for $t \in \mathbb{R}$. Here, $F_i^*(t) = \mathbb{P}(y_i \leq t)$ represents the cumulative distribution function (CDF) at a specified t for each observation y_i .

In this paper, we will explore different structural constraints to estimate $F^*(t)$. These constraints not only ensure interpretable and robust estimators but also prevent overfitting, making them essential in domains such as signal processing, medical diagnostics, and probabilistic weather forecasting. For example, in survival analysis, monotonicity reflects the cumulative nature of survival probabilities, while in genomics, smoothness helps capture gradual trends in gene expression data [Barlow et al. \(1972\)](#); [Tibshirani \(2014\)](#).

To rigorously evaluate the quality of the estimators, we employ the continuous ranked probability Score (CRPS), a widely used metric for assessing the accuracy of probabilistic forecasts [Gneiting and Raftery \(2007\)](#). By quantifying the distance between the estimated and true CDFs, CRPS provides an interpretable and robust framework for comparing estimators under various structural constraints.

1.1 Summary of Results

We now provide a brief summary of the contributions in this paper.

Unified Framework for Estimation: We study a unified framework for estimating $F^*(t)$ by minimizing a quadratic loss over a convex set $K_t \subset \mathbb{R}$. The convex set $K_t \subset \mathbb{R}$ enforces structural constraints on the parameter $F^*(t)$. For the resulting estimator, we provide rigorous theoretical guarantees, including non-asymptotic bounds on both the mean squared error (MSE) and the CRPS.

Applications to Monotonicity and Bounded Variation: We demonstrate the applicability of our framework to convex constraints arising in monotonicity [Brunk \(1969\)](#); [Barlow and Brunk \(1972\)](#); [Chatterjee et al. \(2015\)](#) and bounded total variation [Mammen and Van De Geer \(1997\)](#); [Tibshirani \(2014\)](#); [Guntuboyina et al. \(2020\)](#). These examples illustrate the flexibility and practical utility of the proposed approach for structured parameter estimation.

General Theory for Distributional Regression: We establish a general theory for distributional regression with constraints encoded by arbitrary sets. The main result provides a uniform bound on the empirical ℓ_2 error of $F^*(t)$ across t , with the upper bound explicitly dependent on the approximation error and the complexity of the sets K_t .

Convergence Rates for Neural Networks: Exploiting the general results for arbitrary sets, we derive convergence rates for distributional regression using dense neural networks. This extends the framework of [Kohler and Langer \(2021\)](#) to the context of distributional regression.

1.2 Other Related Work

Distributional regression involves modeling the cumulative distribution function (CDF) of a random variable, whereas quantile regression focuses on estimating the inverse CDF. [Koenker et al. \(2013\)](#) provides a comprehensive review of the distinctions between these two approaches. For instance, if the outcome variable is income and the covariate is a binary variable representing educational attainment, distributional regression would model the probability that income falls below a certain threshold for each educational group. In contrast, quantile regression would estimate income differences between individuals ranked at the same quantile within the two groups. For further discussion on these differences, see also [Peracchi \(2002\)](#).

The approach we adopt in this paper is based on modeling the mean of the random variables of the form $1_{\{y_i \leq t\}}$, which represent the indicator of the events $\{y_i \leq t\}$ for $i = 1, \dots, n$. This idea was first introduced in [Foresi and Peracchi \(1995\)](#) and has since been explored in various contexts, including [Firpo and Sunao \(2023\)](#), [Rothe \(2012\)](#), [Rothe and Wied \(2013\)](#), and [Chernozhukov et al. \(2013\)](#).

More recently, distributional regression has been studied in diverse settings, such as isotonic regression [Henzi et al. \(2021\)](#), random forests [Cevid et al. \(2022\)](#), and neural networks [Shen and Meinshausen \(2024\)](#); [Imani and White \(2018\)](#). These works highlight the versatility and applicability of distributional regression across a range of methodologies and problem domains.

Finally, other nonparametric approaches to distributional regression include [Dunson et al. \(2007\)](#) and [Hall et al. \(1999\)](#).

1.3 Notation

For an event A , we denote by 1_A its indicator, which takes value 1 if A holds and zero otherwise. Throughout, for a vector $v \in \mathbb{R}^n$, we denote by $\|v\|$ and $\|v\|_1$ the ℓ_2 and ℓ_1 norms, respectively. Thus, $\|v\| = \sqrt{\sum_{i=1}^n v_i^2}$ and $\|v\|_1 = \sum_{i=1}^n |v_i|$. Furthermore, given two functions $G, H : \mathbb{R} \rightarrow \mathbb{R}$, we define

$$\text{CRPS}(G, H) = \int_{-\infty}^{\infty} (G(t) - H(t))^2 dt.$$

Also, for $\eta > 0$ and $v \in \mathbb{R}^n$, we write

$$B_\eta(v) := \{u \in \mathbb{R}^n : \|v - u\| \leq \eta\}.$$

For a metric space (\mathcal{X}, d) , let K be a subset of \mathcal{X} , and $r > 0$ be a positive number. Let $B_r(x, d)$ be the ball of radius r with center $x \in \mathcal{X}$. We say that a subset $C \subset \mathcal{X}$ is an r -external covering of K if

$$K \subset \cup_{x \in C} B_r(x, d).$$

Then external covering number of K , written as $N(r, K, d)$, is defined as the minimum cardinality of any r -external covering of K . Furthermore, for a function $f : \mathcal{X} \rightarrow \mathbb{R}$, we define its ℓ_∞ norm as $\|f\|_\infty := \sup_{x \in \mathcal{X}} |f(x)|$. Also, for two sequences a_n and b_n , we write $a_n \lesssim b_n$ if $a_n \leq cb_n$ for a positive constant c , and if $a_n \lesssim b_n$ and $b_n \lesssim a_n$, then we write $a_n \asymp b_n$. The indicator function of a set A is denoted as $1_A(t)$, which takes value 1 if $t \in A$ and 0 otherwise. Finally, the indicator of an event A is 1_A which takes value 1 if A holds and 0 otherwise.

1.4 Outline

The paper is organized as follows: Section 2 introduces the methodology for the convex case. In particular, Section 2.1 establishes a unified framework for distributional regression under structural constraints, while Section 2.2 presents an alternative approach using penalized estimators. Sections 2.3 and 2.4 provide concrete examples of convex estimators, focusing on isotonic regression and trend filtering, respectively. Section 3 extends the framework to the non-convex setting. Specifically, Section 3.1 develops the general theory for non-convex estimators, and Section 3.2 explores an estimator based on deep neural networks. Section 4 presents simulation studies and real-data experiments, comparing the proposed methods to state-of-the-art competitors. Section 4.2 applies the methodology to the Chicago crime dataset. Finally, Section 5 concludes with a

discussion of future research directions, and the Appendix provides additional theoretical results and experimental findings, including two additional real-data applications.

2 Risk Bounds for the Convex Case

2.1 General Result for Constrained Estimators

We begin this section by addressing general problems in distributional regression under convex structural constraints. Specifically, using the notation introduced in Section 1, let $K_t \subset \mathbb{R}^n$ be a convex set, and assume that $F^*(t) \in K_t$. As an initial estimator for $F^*(t)$ consider the following construction. Define the vector

$$w(t) = (1_{\{y_1 \leq t\}}, \dots, 1_{\{y_n \leq t\}})^\top \in \mathbb{R}^n.$$

Based on this, define the estimator

$$\hat{F}(t) := \arg \min_{\theta \in K_t} \{\|w(t) - \theta\|^2\}. \quad (1)$$

Thus, $\hat{F}(t)$ is the projection $w(t)$ onto the convex set K_t . Importantly, $\hat{F}(t)$ can be computed independently for each $t \in \mathbb{R}$, simplifying the estimation process.

Next, we present results that establish key properties of the estimators $\{\hat{F}(t)\}$. Our first result demonstrates that, although these estimators are derived by minimizing the empirical ℓ_2 loss, they are equivalently minimizing the CRPS. This important equivalence is formalized in the following lemma.

Lemma 1. *Suppose that $K_t = K$ for all t . The functions $\{\hat{F}_i\}_{i=1}^n$ satisfy*

$$\{\hat{F}_i\}_{i=1}^n = \arg \min_{\{F_i\}_{i=1}^n : F(t) \in K \forall t} \sum_{i=1}^n \text{CRPS}(F_i, 1\{y_i \leq \cdot\}),$$

where $F(t) = (F_1(t), \dots, F_n(t))^\top$.

Our next result provides an upper bound on the expected value of CRPS error. This is a consequence of a modified version of Theorem A.1 in Guntuboyina et al. (2020), see Theorem 8 in the Appendix.

Theorem 1. *Suppose that $(0, \dots, 0), (1, \dots, 1) \in K_t$, and*

$$\mathbb{P}(y_i \in \Omega) = 1, \text{ for all } i, \quad (2)$$

and some fixed compact set $\Omega \subset \mathbb{R}$. Then, there exists a constant $C > 0$ such that

$$\mathbb{E} \left(\frac{1}{n} \sum_{i=1}^n \text{CRPS}(\hat{F}_i, F_i^*) \right) \leq \frac{C\eta^2}{n} \quad (3)$$

for every $\eta > 1$ satisfying

$$\sup_{t \in \mathbb{R}} \mathbb{E} \left[\sup_{\theta \in K_t : \|\theta - F^*(t)\| \leq \eta} g^\top (\theta - F^*(t)) \right] \leq \frac{\eta^2}{L} \quad (4)$$

where $g \sim N(0, I_n)$, for a universal constant $L > 0$.

Thus, Theorem 1 establishes that obtaining an upper bound on the expected CRPS error reduces to analyzing the local Gaussian complexity expressed on the left-hand side of (4).

As a direct consequence of Theorem 1, we can derive the same upper bound as in (3) for a rearrangement (see e.g. [Lorentz \(1953\)](#); [Bennett and Sharpley \(1988\)](#)) of a truncated version of \widehat{F}_i , which is non-decreasing by construction. This result is formalized in the following theorem.

Corollary 1. *Suppose that $(0, \dots, 0), (1, \dots, 1) \in K_t = K$ for all $t \in \mathbb{R}$, and that $F_i^*(\cdot)$ is continuous for all i . Given $i \in \{1, \dots, n\}$, let $\widehat{F}_i^+(t) = \max\{0, \widehat{F}_i(t)\}$. Let $y_{(1)} \leq \dots \leq y_{(n)}$ be the order statistics of y . Define $a_{i,j} = \widehat{F}_i^+(y_{(j)})$ for $j = 1, \dots, n-1$ and sort the vector $a_{i,\cdot}$ as*

$$a_{i,j_1} \geq \dots \geq a_{i,j_{n-1}},$$

and let \widetilde{F}_i be defined as

$$\widetilde{F}_i(t) = \begin{cases} 0 & \text{if } t < y_{(1)} \\ \sum_{l=1}^{n-1} a_{i,j_l} 1_{[v_l, v_{l-1})}(t) & \text{if } y_{(1)} \leq t < y_{(n)} \\ 1 & \text{if } y_{(n)} \leq t, \end{cases}$$

where $v_0 = y_{(n)}$ and

$$v_l = y_{(n)} - \sum_{k=1}^l (y_{(j_k+1)} - y_{(j_k)})$$

for $l = 1, \dots, n-1$. Then, with the notation from Theorem 1, we have that

$$\mathbb{E} \left(\frac{1}{n} \sum_{i=1}^n \text{CRPS}(\widetilde{F}_i, F_i^*) \right) \leq \frac{C\eta^2}{n}.$$

We conclude this section with a high-probability guarantee that provides an upper bound on the mean squared error for estimating $F^*(t)$, holding uniformly across all t .

Theorem 2. *Suppose that $K_t \subset K$ for all t . For any $\eta > 0$ it holds that*

$$\begin{aligned} & \mathbb{P} \left(\sup_{t \in \mathbb{R}} \sum_{i=1}^n \left(\widehat{F}_i(t) - F_i^*(t) \right)^2 > 2\eta^2 \right) \\ & \leq \frac{C}{\eta^2} \int_0^{\eta/4} \sqrt{\log N(\varepsilon, (K - K) \cap B_\varepsilon(0), \|\cdot\|)} d\varepsilon \\ & + \frac{C\sqrt{\log n}}{\eta}, \end{aligned} \tag{5}$$

for a positive constant C .

Thus, to provide a uniform upper bound on the MSE for estimating $F^*(t)$, it suffices to upper bound the local entropy of $K - K$ where K is an upper set that contains the sets K_t .

2.2 General Result for Penalized Estimators

A natural alternative to shape-constrained estimators is the use of penalized estimators, where the penalty term promotes a desired behavior in the signal being estimated. Motivated by this approach, we present a general result for distributional regression using penalized estimators in this subsection. Specifically, consider estimators of the form

$$\hat{F}(t) := \arg \min_{\theta \in \mathbb{R}^n} \left\{ \frac{1}{2} \|w(t) - \theta\|^2 + \lambda_t \text{pen}_t(\theta) \right\}, \quad (6)$$

where $\lambda_t > 0$ is a tuning parameter and $\text{pen} : \mathbb{R}^n \rightarrow \mathbb{R}$ is a penalty function.

We now present our main result for the penalized estimator defined in (6).

Theorem 3. *Suppose that $\text{pen}_t(\cdot)$ is convex for all t and*

- $\text{pen}_t(v) \geq 0$ for all $v \in \mathbb{R}^n$.
- $\text{pen}_t(\kappa v) = |\kappa| \text{pen}_t(v)$ for all $v \in \mathbb{R}^n$ and $\kappa \in \mathbb{R}$.
- $\text{pen}_t(v + u) \leq \text{pen}_t(v) + \text{pen}_t(u)$ for all $u, v \in \mathbb{R}^n$.

In addition, assume that

$$\sup_{t \in \mathbb{R}} \text{pen}_t(F^*(t)) \leq V.$$

Let $K := \{\theta \in \mathbb{R}^n : \text{pen}_t(\theta) \leq 6V\}$. Then for any $\eta > 0$, it holds that

$$\begin{aligned} & \mathbb{P} \left(\sup_{t \in \mathbb{R}} \sum_{i=1}^n (\hat{F}_i(t) - F_i^*(t))^2 > 2\eta^2 \right) \\ & \leq \frac{C}{\eta^2} \int_0^{\eta/4} \sqrt{\log N(\varepsilon, K \cap B_\varepsilon(0), \|\cdot\|)} d\varepsilon + \frac{C\sqrt{\log n}}{\eta}, \end{aligned} \quad (7)$$

for some constant $C > 0$, provide that we set $\lambda_t = \eta^2 / 4\text{pen}(F^*(t))$.

Theorem 3 demonstrates that achieving a uniform upper bound on the MSE can be accomplished by controlling the covering number of sets of the form $K \cap B_\varepsilon(0)$, as outlined on the right-hand side of (7).

2.3 Isotonic Regression

In this subsection, we focus on distributional isotonic regression, a topic that has received considerable attention in the literature [Davidov and Iliopoulos \(2012\)](#); [El Barmi and Mukerjee \(2005\)](#); [Hogg \(1965\)](#); [Jiménez and El Barmi \(2003\)](#). The most relevant works to our results are [Mösching and Dümbgen \(2020\)](#), which examined distributional isotonic regression under smoothness constraints, and [Henzi et al. \(2021\)](#), which proposed an interpolation method equivalent to the formulation in (1) with K_t enforcing a monotonicity constraint.

Setting

$$K_t = K := \{\theta \in \mathbb{R}^n : \theta_1 \leq \theta_2 \leq \dots \leq \theta_n\}, \quad (8)$$

we now consider the case of isotonic distributional regression assuming that $F^*(t) \in K_t$, which is equivalent to $\mathbb{P}(Y_1 \leq t) \leq \dots \leq \mathbb{P}(Y_n \leq t)$.

With the constraint sets as in (8), the resulting estimator in (1) can be found with the pool adjacent violators algorithm from [Robertson \(1988\)](#).

Theorem 4. Consider the estimators $\{\hat{F}_t\}_{t \in \mathbb{R}}$ defined in (1) with K_t defined as (8). If $F^*(t) \in K$ and (2) holds for some fixed compact set Ω , then

$$\mathbb{E} \left(\frac{1}{n} \sum_{i=1}^n \text{CRPS}(\hat{F}_i, F_i^*) \right) \leq Cn^{-2/3}, \quad (9)$$

for some positive constant $C > 0$. Moreover, (9) holds replacing \hat{F} with the corresponding \tilde{F} as defined in Corollary 1, provided that each function F_i^* is continuous. Finally, if $K_t = K \cap [a, b]$ with K as in (8), then

$$\sup_{t \in \mathbb{R}} \sum_{i=1}^n \frac{1}{n} \left(\hat{F}_i(t) - F_i^*(t) \right)^2 = O_{\mathbb{P}} \left(\frac{(b-a)^{2/3}}{n^{2/3}} + \frac{\log n}{n} \right), \quad (10)$$

where (10) holds without requiring (2) nor continuity of the F_i^* 's.

The result in Theorem 4 establishes that distributional isotonic regression achieves an estimation rate of $n^{-2/3}$ for both the expected average CRPS and the worst-case MSE, as in (10). This result improves upon Theorem 3 in Henzi et al. (2021), which only demonstrated convergence in probability for isotonic distributional regression.

2.4 Trend Filtering

In this subsection, we focus on distributional regression under a total variation constraint. Total variation-based methods were independently introduced by Rudin et al. (1992), Mammen and Van De Geer (1997), and Tibshirani et al. (2005). These methods have been extensively studied in various contexts within the statistics literature, including univariate settings Tibshirani (2014); Lin et al. (2017); Guntuboyina et al. (2020); Madrid Padilla and Chatterjee (2022); Padilla et al. (2023), grid graphs Hütter and Rigollet (2016); Chatterjee and Goswami (2021), and general graphs Wang et al. (2016); Padilla et al. (2018).

Before establishing our proposed total variation estimators, we introduce some additional notation. For a vector $\theta \in \mathbb{R}^n$, define $D^{(0)}(\theta) = \theta$, $D^{(1)}(\theta) = (\theta_2 - \theta_1, \dots, \theta_n - \theta_{n-1})^\top$ and $D^{(r)}(\theta)$, for $r \geq 2$, is recursively defined as $D^{(r)}(\theta) = D^{(1)}(D^{(r-1)}(\theta))$, where $D^{(r)}(\theta) \in \mathbb{R}^{n-r}$. With this notation, for $r \geq 1$, the r th order total variation of a vector θ is given as

$$\text{TV}^{(r)}(\theta) = n^{r-1} \|D^{(r)}(\theta)\|_1. \quad (11)$$

The concept of the r th total variation can be understood as follows. Consider θ as the evaluations of an r times differentiable function $f : [0, 1] \rightarrow \mathbb{R}$ on the grid $(1/n, 2/n, \dots, n/n)$. In this case, a Riemann approximation of the integral $\int_{[0,1]} |f^{(r)}(t)| dt$ corresponds precisely to $\text{TV}^{(r)}(\theta)$, where $f^{(r)}$ denotes the r th derivative of f . Therefore, for natural instances of θ , it is reasonable to expect that $\text{TV}^{(r)}(\theta) = O(1)$.

The above discussion motivates us to define the sets

$$K_t := \left\{ \theta \in \mathbb{R}^n : \text{TV}^{(r)}(\theta) \leq V_t \right\}, \quad (12)$$

for some $V_t > 0$, and consider the corresponding estimator in (1). The intuition here is that if $F^*(t) \in K_t$ then the probabilities $F_1^*(t), \dots, F_n^*(t)$ change smoothly over i in the sense that $F^*(t)$

has bounded r th total variation. The resulting set in (12) allows us to define the trend filtering distributional regression estimator subject of our next theorem which follows from the results in Section 2.1.

Theorem 5. *Consider the estimator in (1) with K_t as in (12) for an integer r satisfying $r \geq 1$. If $F^*(t) \in K_t$, (2) holds for some fixed compact set Ω , and $\sup_t V_t \leq V$, then*

$$\mathbb{E} \left(\frac{1}{n} \sum_{i=1}^n \text{CRPS}(\widehat{F}_i, F_i^*) \right) \leq C \left[\frac{V^{\frac{2}{2r+1}}}{n^{\frac{2r}{2r+1}}} + \frac{\log n}{n} \right] \quad (13)$$

for a positive constant C . Moreover, the upper bound in (13) also holds for the corresponding sorted estimators \widetilde{F}_i as defined in Corollary 1, provided that each function F_i^* is continuous and $V_t = V$ for all t . Finally,

$$\sup_{t \in \mathbb{R}} \sum_{i=1}^n \frac{1}{n} (\widehat{F}_i(t) - F_i^*(t))^2 = O_{\mathbb{P}} \left(\frac{V^{\frac{2}{2r+1}}}{n^{\frac{2r}{2r+1}}} + \frac{\log n}{n} \right), \quad (14)$$

where (14) holds without requiring (2), constant V_t , nor continuity of the F_i^* 's.

We now turn to a statistical guarantee for the penalized version of trend filtering in distributional regression. This result follows directly from Theorem 3 and involves a calculation analogous to the proof of (14).

Corollary 2. *Consider the estimator in (6) with $\text{pen}_t(\theta) := \text{TV}^{(r)}(\theta)$ and λ_t chosen as in Theorem 3. Then*

$$\sup_{t \in \mathbb{R}} \sum_{i=1}^n \frac{1}{n} (\widehat{F}_i(t) - F_i^*(t))^2 = O_{\mathbb{P}} \left(\frac{V^{\frac{2}{2r+1}}}{n^{\frac{2r}{2r+1}}} + \frac{\log n}{n} \right), \quad (15)$$

where $V := \sup_{t \in \mathbb{R}} \text{pen}_t(F^*(t))$.

Theorem 5 establishes that the constrained version of trend filtering for distributional regression achieves the rate $V^{1/(2r+1)} n^{-2r/(2r+1)}$, ignoring logarithmic factors, for both the CRPS and the worst-case MSE. This result aligns with the convergence rate of trend filtering in one-dimensional regression, where the same rate is attained when the regression function has r th-order total variation Mammen and Van De Geer (1997); Tibshirani (2014); Guntuboyina et al. (2020). Additionally, per Corollary 2, the penalized version of trend filtering for distributional regression achieves the same rate in terms of the worst-case MSE, further reinforcing its consistency with classical trend filtering results.

3 Risk Bounds for the General Case

3.1 General Result

This subsection aims to present our main result on constrained distributional regression in scenarios where the constraint sets K_t are arbitrary, not necessarily convex, and potentially misspecified for $F^*(t)$.

Theorem 6. Let $\widehat{F}(t)$ be the estimator defined in (1) for all $t \in \mathbb{R}$ but with K_t not necessarily convex and with $F^*(t)$ not necessarily in K_t . Suppose that

$$\sup_{t \in \mathbb{R}} \sup_{F(t) \in K_t} \|F(t)\|_\infty \leq B$$

for some constant $B \geq 1$, and $K_t \subset K$ for all t and some set K . Let $G(t)$ be defined as

$$G(t) \in \arg \min_{F(t) \in K_t} \|F(t) - F^*(t)\|_\infty.$$

Then, for $\eta > 1$, with $K(\varepsilon) = (K - K) \cap B_\varepsilon(0)$, we have that

$$\begin{aligned} & \mathbb{P} \left(\sup_{t \in \mathbb{R}} \|\widehat{F}(t) - F^*(t)\| > \eta + \sup_{t \in \mathbb{R}} \sqrt{n} \|F^*(t) - G(t)\|_\infty \right) \\ & \leq \frac{C}{\eta^2} \sum_{j=1}^J \frac{1}{2^{j-2}} \int_0^{2^{j/2}\eta/4} \sqrt{\log N(\varepsilon, K(\varepsilon), \|\cdot\|)} d\varepsilon + \\ & \quad \frac{C\sqrt{\log n}}{\eta} + \frac{C\sqrt{n}}{\eta} \sup_{t \in \mathbb{R}} \|G(t) - F^*(t)\|_\infty \end{aligned}$$

for some positive constant $C > 0$, and where

$$J = \left\lceil \frac{\log(2nB/\eta^2)}{\log 2} \right\rceil.$$

The proof of Theorem 6, provided in Appendix B.7, relies on a peeling argument and extends ideas originally developed for the convex case. The intuition behind Theorem 6 is that η can be interpreted as the estimation error, which is chosen based on the covering number of the sets $K(\varepsilon)$. The second term, $\sup_{t \in \mathbb{R}} \sqrt{n} \|F^*(t) - G(t)\|_\infty$, represents the approximation error, capturing the mismatch between the signal class K_t and the true $F^*(t)$. This decomposition highlights the balance between estimation accuracy and model misspecification.

3.2 Dense ReLU Networks

We now turn to the application of Theorem 6 to the problem of distributional regression using dense neural networks. The results in this section add to the literature on statistical theory for rectified linear unit (ReLU) networks as in Bauer and Kohler (2019); Schmidt-Hieber (2020); Kohler and Langer (2021); Padilla et al. (2022); Ma and Safikhani (2022); Zhang et al. (2024); Padilla et al. (2024).

Before presenting our main result, we first revisit some key notation from Kohler and Langer (2021). Suppose we are given independent data $\{(x_i, y_i)\}_{i=1}^n \subset [0, 1]^{d_0} \times \mathbb{R}$ and let

$$G^*(x, t) := \mathbb{P}(y_i \leq t | x_i = x) = f_t^*(x) \tag{16}$$

for functions $f_t^*[0, 1]^{d_0} \rightarrow \mathbb{R}$ for all t . We set $F_i^*(t) = G^*(x_i, t)$.

To proceed, we first define the constraint set K_t before outlining the assumptions on $F^*(t)$. To that end, we describe a dense neural network with architecture (L, k) employing the ReLU

activation function given as $\rho(s) = \max\{0, s\}$ for any $s \in \mathbb{R}$. Such a network is represented as a real-valued function $f : \mathbb{R}^d \rightarrow \mathbb{R}$ satisfying the following properties:

$$f(x) = \sum_{i=1}^{k_L} c_{1,i}^{(L)} f_i^{(L)}(x) + c_{1,0}^{(L)} \quad (17)$$

for weights $c_{1,0}^{(L)}, \dots, c_{1,k_L}^{(L)} \in \mathbb{R}$ and for $f_i^{(L)}$'s recursively defined by

$$f_i^{(s)}(x) = \rho \left(\sum_{j=1}^{k_{s-1}} c_{i,j}^{(s-1)} f_j^{(s-1)}(x) + c_{i,0}^{(s-1)} \right) \quad (18)$$

for some $c_{i,0}^{(s-1)}, \dots, c_{i,k_{s-1}}^{(s-1)} \in \mathbb{R}$, $s \in \{2, \dots, L\}$, and $f_i^{(1)}(\mathbf{x}) = \rho \left(\sum_{j=1}^d c_{i,j}^{(0)} x^{(j)} + c_{i,0}^{(0)} \right)$ with $c_{i,0}^{(0)}, \dots, c_{i,d}^{(0)} \in \mathbb{R}$.

Proceeding as in [Kohler and Langer \(2021\)](#), we suppose that all hidden layers possess an identical number of neurons and define $\mathcal{F}(L, \nu)$ as the set of functions f of the form (17) and (18), with $k_1 = \dots = k_L = \nu$, and $\|f\|_\infty \leq 1$. Then, we let

$$K_t = K := \left\{ \theta \in \mathbb{R}^n : \theta_i = f(x_i) \text{ } i = 1, \dots, n, \text{ for some } f \in \mathcal{F}(L, \nu) \right\}. \quad (19)$$

Next we provide some notation necessary for define the class of signals where the $F^*(t)$'s belong.

Definition 1 ((p, C)-smoothness). Let $p = q + s$ for some $q \in \mathbb{N} = \mathbb{Z}^+ \cup \{0\}$ and $0 < s \leq 1$. We say that a function $g : \mathbb{R}^d \rightarrow \mathbb{R}$ is (p, C) -smooth, if for every $\alpha = (\alpha_1, \dots, \alpha_d) \in \mathbb{N}^d$, with $d \in \mathbb{Z}^+$, where $\sum_{j=1}^d \alpha_j = q$, the partial derivative $\partial^q g / (\partial u_1^{\alpha_1} \dots \partial u_d^{\alpha_d})$ exists and

$$\left| \frac{\partial^q g}{\partial u_1^{\alpha_1} \dots \partial u_d^{\alpha_d}}(u) - \frac{\partial^q g}{\partial u_1^{\alpha_1} \dots \partial u_d^{\alpha_d}}(v) \right| \leq C \|u - v\|^s$$

for all $u, v \in \mathbb{R}^d$.

Let us now define the generalized hierarchical interaction models $\mathcal{H}(l, \mathcal{P})$.

Definition 2 (Space of Hierarchical Composition Models, [Kohler and Langer \(2021\)](#)). For $l = 1$ and smoothness constraint $\mathcal{P} \subseteq (0, \infty) \times \mathbb{N}$, the space of hierarchical composition models is defined as

$$\begin{aligned} \mathcal{H}(1, \mathcal{P}) := \\ \left\{ h : \mathbb{R}^d \rightarrow \mathbb{R} : h(a) = m(a_{(\pi(1))}, \dots, a_{(\pi(M))}), \text{ where} \right. \\ \left. m : \mathbb{R}^M \rightarrow \mathbb{R} \text{ is } (p, C)\text{-smooth for some } (p, M) \in \mathcal{P} \right. \\ \left. \text{and } \pi : \{1, \dots, M\} \rightarrow \{1, \dots, d\} \right\}. \end{aligned}$$

For $l > 1$, we set

$$\begin{aligned} \mathcal{H}(l, \mathcal{P}) := \\ \left\{ h : \mathbb{R}^d \rightarrow \mathbb{R} : h(\mathbf{x}) = m(f_1(a), \dots, f_M(a)), \text{ where} \right. \\ \left. m : \mathbb{R}^M \rightarrow \mathbb{R} \text{ is } (p, C)\text{-smooth for some } (p, M) \in \mathcal{P} \right. \\ \left. \text{and } f_i \in \mathcal{H}(l-1, \mathcal{P}) \right\}. \end{aligned}$$

With the notation above, we are ready to state our assumption on the true signals in the spirit of Kohler and Langer (2021).

Assumption 1. Suppose that for all t the function $G^*(\cdot, t)$ is in the class $\mathcal{H}(l, \mathcal{P})$ as in Definition 2. In addition, assume that each function g^t in the definition of $G^*(\cdot, t)$ can have different smoothness $p_{g^t} = q_{g^t} + s_{g^t}$, for $q_{g^t} \in \mathbb{N}$, $s_{g^t} \in (0, 1]$, and of potentially different input dimension M_{g^t} , so that $(p_{g^t}, M_{g^t}) \in \mathcal{P}$. Let M_{\max} be the largest input dimension and p_{\max} the largest smoothness of any of the functions g^t for all t . Suppose that for each g^t all the partial derivatives of order less than or equal to q_{g^t} are uniformly bounded by constant C_{Smooth} , and each function g^t is Lipschitz continuous with Lipschitz constant $C_{\text{Lip}} \geq 1$. Also, assume that $\max\{p_{\max}, M_{\max}\} = O(1)$.

We now present our main result concerning distributional regression with ReLU neural networks.

Theorem 7. Let $\widehat{F}(t)$ be the estimator from (1) with the set K_t as in (19) for all $t \in \mathbb{R}$ with $F^*(t)$ not necessarily in K_t . Suppose that Assumption 1 holds. Let

$$\phi_n = \max_{(p, M) \in \mathcal{P}} n^{\frac{-2p}{(2p+M)}}.$$

There exists positive constants c_1 and c_2 such that if

$$L = \lceil c_1 \log n \rceil \quad \text{and} \quad \nu = \left\lceil c_2 \max_{(p, M) \in \mathcal{P}} n^{\frac{M}{2(2p+M)}} \right\rceil \quad (20)$$

or

$$L = \left\lceil c_1 \max_{(p, M) \in \mathcal{P}} n^{\frac{M}{2(2p+M)}} \log n \right\rceil \quad \text{and} \quad \nu = \lceil c_2 \rceil, \quad (21)$$

then

$$\sup_{t \in \mathbb{R}} \sum_{i=1}^n \frac{1}{n} \left(\widehat{F}_i(t) - F_i^*(t) \right)^2 = O_{\mathbb{P}} \left(\frac{\log n}{n} + \phi_n \log^4 n \right). \quad (22)$$

Theorem 7 demonstrates that dense ReLU neural network estimators for distributional regression uniformly achieve the rate ϕ_n , up to logarithmic factors, in terms of the worst-case MSE for estimating the true parameters $\{F^*(t)\}_{t \in \mathbb{R}}$, provided these parameters belong to a hierarchical composition class. Importantly, this rate aligns with the results of Kohler and Langer (2021), which established the same rate for regression function estimation in the hierarchical composition class under sub-Gaussian error assumptions.

4 Experiments

4.1 Simulated Data Analysis

We evaluate the performance of the proposed methods against state-of-the-art approaches across diverse simulation settings that reflect various practical challenges and structural assumptions. Specifically, six distinct scenarios are considered to evaluate different aspects of the distributional regression problem.

We refer to our proposed approach as **UnifDR**, which adapts different methods based on the scenario. In the first two scenarios, **UnifDR** applies the isotonic regression method described in Section 2.3.

- **Scenario 1 (S1).** We generate data $y_i \sim \text{Normal}(\mu_i, 1)$ where $\mu_i = 1 - i/n$ for $i = 1, \dots, n$. Ensuring monotonicity in the CDFs.
- **Scenario 2 (S2).** We consider $y_i \sim \text{Unif}(a_i, b_i)$, where $a_i = (n - i)/n$ and $b_i = a_i + 1$, which also guarantees monotonicity in the CDFs.

In the next two scenarios **UnifDR** uses the trend filtering method described in Section 2.4.

- **Scenario 3 (S3).** The true CDFs are modeled as $F_i^*(t) = \text{Exp}(\mu_i)$, where $\mu_i = 1 + 0.5 \sin(2\pi i/n)$.
- **Scenario 4 (S4).** Consider $F_i^*(t) = \text{Gamma}(\text{shape} = 0.7, \text{scale} = \mu_i)$, where the scale parameter follows a piecewise constant pattern as a function of i ,

$$\mu_i = 6 \cdot 1_{\{i \leq n/4\}} + 2 \cdot 1_{\{n/4 < i \leq n/2\}} + 8 \cdot 1_{\{n/2 < i \leq 3n/4\}} + 4 \cdot 1_{\{i > 3n/4\}}.$$

For the last two scenarios **UnifDR** utilizes the Dense ReLU Networks method, described in Section 3.2,

- **Scenario 5 (S5).** Let $\mathbf{x}_i \sim \text{Unif}([0, 1]^5)$ be generated independently. The true CDFs are given by $F_i^*(t) = \Phi((t - h(\mathbf{x}_i))/0.5)$, where

$$h(\mathbf{x}_i) = -3x_i^{(1)} + 2 \log(1 + x_i^{(2)}) + x_i^{(3)} + 5x_i^{(4)} + (x_i^{(5)})^2.$$

The function Φ represents the standard normal cumulative distribution function.

- **Scenario 6 (S6).** The covariates \mathbf{x}_i are independently drawn from $\text{Unif}([0, 1]^{10})$. The response values y_i follow a Chi-square distribution with a degrees of freedom parameter given by $y_i \sim \chi^2(h(\mathbf{x}_i))$. The function $h(\mathbf{x}_i)$ is specified as

$$h(\mathbf{x}_i) = \log \left(\left| -0.5 \cdot \sum_{j=1}^3 \sin(\pi x_i^{(j)}) - 0.5 \sum_{j=4}^9 x_i^{(j)} + 0.5 \cos(x_i^{(10)}) \right| + 2 \right).$$

To implement our proposed approach **UnifDR** we proceed as follows. The isotonic method introduced in Section 2.3 is implemented in R using the pool adjacent violators algorithm (PAVA) from Robertson (1988). For this approach there are no direct competitors in the distributional regression problem.

The Trend Filtering estimator in Section 2.4 is implemented using the `trendfilter` function from the `glmgen` package in R, and we compare it with additive smoothing splines (ASS) via the `smooth.spline` function in R.

For the Dense ReLU Networks method in Section 3.2, we use a fully connected feedforward architecture with an input layer, two hidden layers (64 units each), and an output layer. The network is implemented in Python and trained using the Adam optimizer with a learning rate of 0.001. In this case, we compare the proposed UnifDR method with five benchmark methods. First, we consider Classification and Regression Trees (CART) (Breiman et al., 1984), implemented in R via the `rpart` package, with the complexity parameter used for tuning. Second, we evaluate Multivariate Adaptive Regression Splines (MARS) (Friedman, 1991), available in the `earth` package,

where the penalty parameter serves as the tuning parameter. Third, we assess Random Forests (RF) (Breiman, 2001), implemented in R via the `randomForest` package, using 500 trees and tuning the minimum terminal node size. Additionally, we consider two recent methods. Distributional Random Forests (DRF) (Civid et al., 2022) is implemented via the `drf` package in Python. DRF employs tree-based ensembles with tuning parameters including the splitting rule and the number of trees. Lastly, Engression (EnG) (Shen and Meinshausen, 2024) is implemented using the `engression` package in Python. EnG utilizes hierarchical structured neural networks and we adopt the same training hyperparameters as our deep learning approach to ensure optimization consistency. EnG also requires a sampling procedure, with the number of samples set to 1000 for accurate distribution estimation.

Performance Evaluation: For each scenario, datasets with sample sizes $n \in \{400, 800, 1600\}$ are generated, with each experiment repeated 100 times using Monte Carlo simulations. Evaluations are conducted at 100 evenly spaced points t from three fixed intervals: $\Lambda_1 = [-1, 0.4]$, $\Lambda_2 = [-2, 2]$, and $\Lambda_3 = [0.8, 10]$. Each dataset is randomly split into 75% training and 25% test sets. Competing models undergo 5-fold cross-validation on the training data for hyperparameter tuning, with performance assessed on the test set.

For the isotonic regression method, test set predictions are obtained via naive nearest neighbor interpolation.

The accuracy of the estimated CDFs $\hat{F}_i(t)$ relative to the true CDFs $F_i^*(t)$ is evaluated using the following performance metrics, averaged over 100 Monte Carlo repetitions.

- **CRPS:** CRPS evaluates the overall fit of $\hat{F}_i(t)$ to $F_i^*(t)$ across all evaluation points in \mathbb{R} . Since evaluation is performed over a finite set of 100 values in Λ , CRPS is approximated via a Riemann sum: $\text{CRPS} = \frac{1}{|\text{Test}|} \sum_{i \in \text{Test}} \frac{1}{100} \sum_{t \in \Lambda} \left(\hat{F}_i(t) - F_i^*(t) \right)^2$, where $|\text{Test}| = \frac{n}{4}$ is the size of the test set.
- **Maximum Squared Difference (MSD):** MSD captures the worst-case discrepancy between $\hat{F}_i(t)$ and $F_i^*(t)$, approximated as: $\text{MSD} = \max_{t \in \Lambda} \frac{1}{|\text{Test}|} \sum_{i \in \text{Test}} \left(\hat{F}_i(t) - F_i^*(t) \right)^2$.

The results below focus on the CRPS metric for Scenarios **S1** through **S6**, evaluated on Λ_2 . Appendix A provides additional results, including MSD performance across all evaluation sets and CRPS evaluations for Λ_1 and Λ_3 .

Figure 3 presents the performance of **UnifDR** in **S1** and **S2**, where it employs isotonic regression with no direct competitors. The same figure also includes results for **S3** and **S4**, where **UnifDR** applies the Trend Filtering method and is compared to ASS. Additionally, results for **S5** are shown in this same figure, where **UnifDR** utilizes the Dense ReLU Networks method against five state-of-the-art competitors: CART, MARS, RF, DRF, and EnG. Figure 1 presents results for **S6**, analyzed under the same framework as **S5**.

In all scenarios, **UnifDR** consistently outperforms competing methods, with its performance superiority becoming more pronounced as the sample size increases. This dominance is further confirmed by the extended evaluations in Appendix A, reinforcing the robustness of **UnifDR** across various conditions.

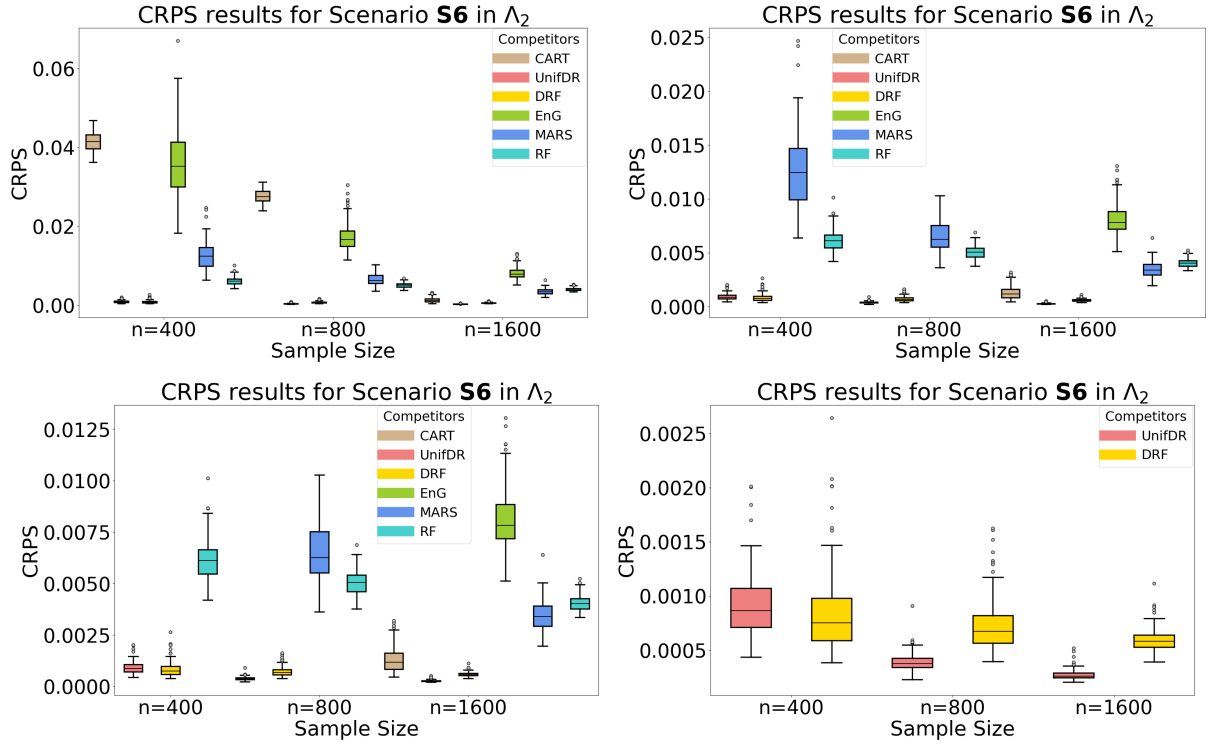


Figure 1: Box plots for CRPS results for **S6** in Λ_2 . The top row shows results for all the competitors (left) and, competitors with median below 0.02 (right). The bottom row displays results for competitors with median below 0.01 (left), and best two competitors (right).

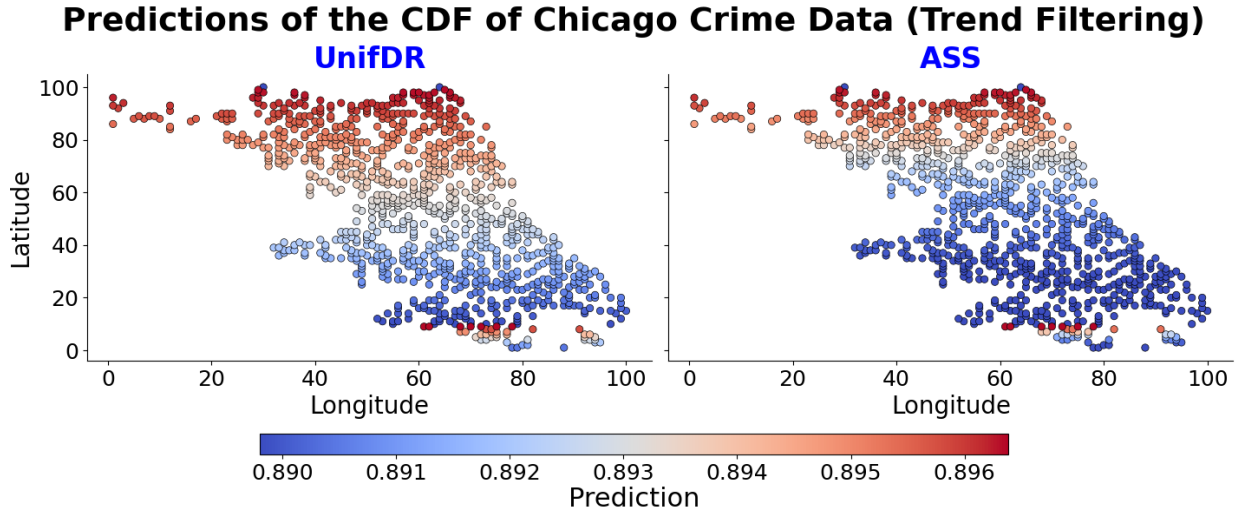


Figure 2: $\widehat{F}_i(t)$ for $t = 3$ and all $i \in \text{Test}$, for all competitors.

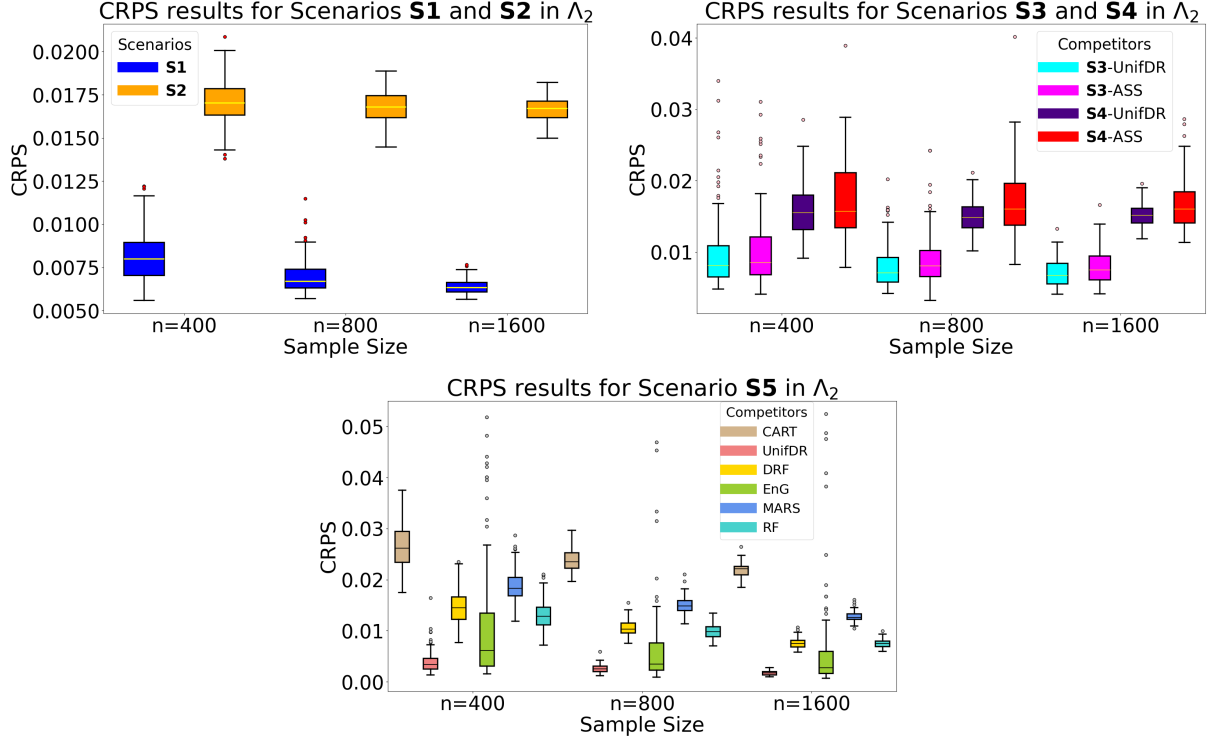


Figure 3: Box plots of CRPS results for all competitors in Λ_2 . The top row (left) corresponds to **S1** and **S2**, while the top row (right) represents **S3** and **S4**. The bottom row displays the results for **S5**.

4.2 Real data application

In this section, we evaluate the performance of the proposed **UnifDR** method using both the Trend Filtering and Dense ReLU network procedures on real-world datasets.

4.2.1 Chicago Crime Data

We analyze the 2015 Chicago crime dataset, available at <https://data.gov/open-gov/>, which records reported crimes in Chicago throughout the year. Following [Tansey et al. \(2018\)](#), the spatial domain is discretized into a 100×100 grid, where each grid cell aggregates crime counts within its spatial boundary. The response variable is defined as the log-transformed total crime counts per grid cell. Grid cells with zero observed crimes are excluded, yielding a final dataset of 3,844 grid cells.

We evaluate **UnifDR** using two different approaches: Trend Filtering and Dense ReLU Networks. The Trend Filtering approach does not incorporate covariates, instead, it assumes a smooth index trend, treating the grid cells as an ordered sequence. The ordering is established lexicographically. In contrast, the the Dense ReLU network approach leverages covariate information for modeling crime intensity. The following covariates are included. Latitude and Longitude Bins, encapsulating spatial crime patterns. Day of the Week, encoded as integers (Monday = 2, ..., Sunday = 1). Beat, a categorical identifier for Chicago's policing districts. Arrest Indicator, a binary variable denoting whether an arrest was made (1) or not (0).

For both approaches, the dataset is randomly partitioned into 100 train (75%)–test (25%) splits, and evaluation is conducted at evenly spaced points Λ in the interval $[-1,6]$. The Dense ReLU Networks approach employs a fully connected feedforward architecture with five hidden layers of 64 neurons each, using ReLU activations. The model is trained using the Adam optimizer with a learning rate of 0.001 over 1,000 epochs, minimizing the Binary Cross-Entropy (BCE) loss function for improved CDF estimation.

Performance is assessed using the Continuous Ranked Probability Score (CRPS) and Maximum Squared Difference (MSD) metrics, comparing estimated CDFs $\hat{F}_i(t)$ against empirical indicators $w_i(t)$. Table 1 summarizes the results for the Trend Filtering approach, while Table 2 presents the results for the Dense ReLU Networks approach. The results demonstrate that across both methodologies, **UnifDR** consistently outperforms competing methods, achieving superior predictive accuracy. Furthermore, Figures 2 and 4 provide a visualization of $\hat{F}_i(t)$ at $t = 3$ for all different methods in both settings.

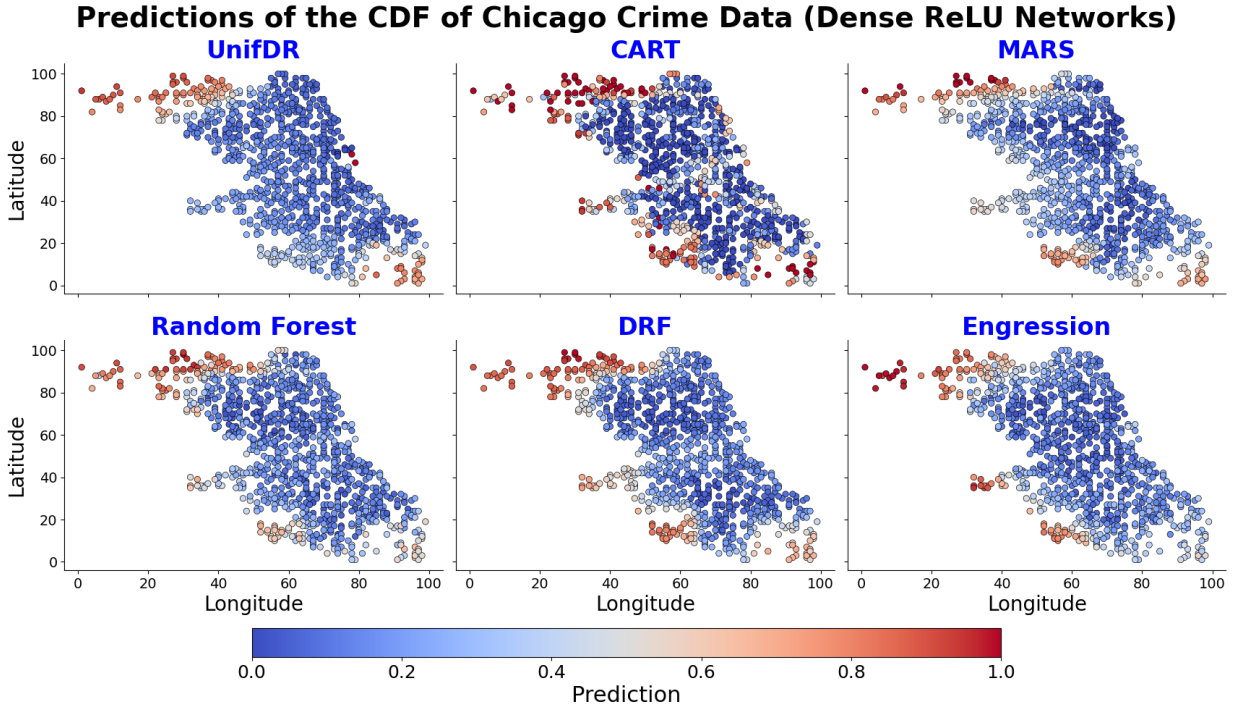


Figure 4: $\hat{F}_i(t)$ for $t = 3$ and all $i \in \text{Test}$, for all competitors.

4.2.2 Other Real Data Examples

Beyond the Chicago crime dataset, **UnifDR** is further evaluated on California housing prices and daily Ozone measurements. Detailed descriptions, pre-processing steps, and results are provided in the Appendix A.1.

Table 1: Evaluation metrics for UnifDR (Trend Filtering approach) and its competitor ASS on the 2015 Chicago crime dataset.

METHOD	CRPS (MEAN \pm STD)	MSD (MEAN \pm STD)
UNIFDR	0.0976\pm0.0017	0.2509\pm0.0025
ASS	0.1223 \pm 0.0078	0.2850 \pm 0.0391

Table 2: Evaluation metrics for UnifDR (Dense ReLU networks) and its competitors on the Chicago crime dataset.

METHOD	CRPS (MEAN \pm STD)	MSD (MEAN \pm STD)
UNIFDR	0.0811\pm 0.0018	0.2133 \pm 0.0031
CART	0.0951 \pm 0.0017	0.2622 \pm 0.0071
DRF	0.0906 \pm 0.0018	0.2477 \pm 0.0042
ENG	0.1014 \pm 0.0028	0.2652 \pm 0.0045
MARS	0.0974 \pm 0.0019	0.2732 \pm 0.0047
RF	0.0934 \pm 0.0020	0.2581 \pm 0.0031

5 Conclusion

This paper introduced a unified framework for nonparametric distributional regression under convex and non-convex structural constraints. We established theoretical risk bounds for the estimation of cumulative distribution functions (CDFs) in various settings, including isotonic regression, trend filtering, and deep neural networks. Our analysis leveraged continuous ranked probability scores (CRPS) and worst-case mean squared error (MSE) to quantify estimation accuracy, demonstrating that structured constraints such as monotonicity, bounded total variation, and hierarchical function composition lead to improved estimation accuracy.

Our theoretical results establish explicit convergence guarantees for isotonic, strengthening prior findings. Moreover, the trend filtering estimator achieves rates consistent with classical one-dimensional regression results. For deep neural networks, we show that dense ReLU-based estimators achieve comparable rates under hierarchical composition constraints, aligning with existing results in structured regression. Experiments on simulated and real datasets further validated the theoretical guarantees, with our proposed methods consistently outperforming alternative approaches. In particular, **UnifDR**, our proposed distributional regression framework, demonstrated superior performance across all considered settings.

An important avenue for future research is extending our approach to dependent data settings. Many real-world applications involve time-series data, spatial data, or network-structured data, where dependencies among observations must be accounted for.

A Additional Numerical Results

This appendix provides an extensive evaluation of the proposed methods, **UnifDR**, including additional results and analyses that were omitted from Section 4. These supplementary results further demonstrate the effectiveness and robustness of our methods across diverse settings. The appendix presents:

- Additional real data applications to illustrate the practical utility of the proposed methods (Appendix A.1).
- Comprehensive evaluations on alternative test sets (Λ_1 and Λ_3) supplementing the results for Λ_2 in Section 4.1.
- Performance results based on the Maximum Squared Difference (MSD) metric across all scenarios, which were not included in Section 4.1 (Appendix A.3).

A.1 Additional Real Data Applications

This appendix presents two additional real-world data applications to further demonstrate the effectiveness of the proposed methods. These examples span different domains, illustrating the versatility and robustness of our approach. Each case study includes a description of the dataset, the experimental setup, and a comparative performance analysis.

For both datasets, the empirical cumulative distribution function (CDF), $w_i(t)$, is used to evaluate model performance over 100 evenly spaced points in a predefined range. The performance of the proposed methods is assessed using the Continuous Ranked Probability Score (CRPS) and the Maximum Squared Difference (MSD) metrics, defined as follows:

$$\text{CRPS} = \frac{1}{|\text{Test}|} \sum_{i \in \text{Test}} \frac{1}{100} \sum_{t \in \Lambda} (\hat{F}_i(t) - w_i(t))^2$$

and

$$\text{MSD} = \max_{t \in \Lambda} \frac{1}{|\text{Test}|} \sum_{i \in \text{Test}} (\hat{F}_i(t) - w_i(t))^2$$

Each dataset is randomly divided into a training subset (75%) and testing (25%) subsets. The proposed **UnifDR** method is implemented in two variants: Trend Filtering, which captures smooth variations through total variation regularization, and Dense ReLU Networks, which leverages a deep neural network to incorporate covariate information.

A.1.1 California Housing Prices

We evaluate the effectiveness of the proposed **UnifDR** method by analyzing the 1990 California housing dataset, which contains demographic and economic information from various neighborhoods across California. Originally introduced in Pace and Barry (1997), the dataset comprises 20,640 observations and is publicly available via the Carnegie Mellon StatLib repository at <http://lib.stat.cmu.edu/datasets/>, as well as the https://www.dcc.fc.up.pt/~ltorgo/Regression/cal_housing.html portal.

Following the approach of Ye and Padilla (2021), the geographic area is discretized into a 200×200 spatial grid based on latitude and longitude coordinates. The response variable is derived

Table 3: Evaluation metrics for UnifDR and its competitor ASS on the California housing dataset.

METHOD	CRPS (MEAN \pm STD)	MSD (MEAN \pm STD)
UNIFDR	0.0343 \pm 0.0013	0.2505 \pm 0.0097
ASS	0.0357 \pm 0.0028	0.2652 \pm 0.0407

by applying a logarithmic transformation to the median house values within each grid cell to enhance numerical stability and interpretability. Grid cells lacking valid data are excluded from further analysis, resulting in a final sample size of 3,165 grid cells.

In the Trend Filtering setup, no covariates are included; instead, the spatial grid is treated as an ordered sequence, allowing total variation regularization to capture smooth spatial variations in housing prices. The response variable for each cell of the grid is the median house value transformed by logarithms. In contrast, the Dense ReLU Networks method incorporates both spatial features, such as latitude and longitude, and socioeconomic attributes, including `median_income` and `average_occupancy` (computed as population divided by households), to model the complex relationships influencing housing prices. The Dense ReLU neural network consists of three hidden layers, each with 30 neurons followed by a ReLU activation function.

Evaluations are performed over 100 evenly spaced points within the range [5, 15]. Figure 5 presents the estimated cumulative distribution functions $\hat{F}_i(t)$ at $t = 12$, comparing the performance of **UnifDR** (Trend Filtering) against its competitor, ASS. Similarly, Figure 6 illustrates the estimated cumulative distribution functions at the same evaluation point, this time comparing **UnifDR** (Dense ReLU networks) against CART, MARS, RF, DRF, and EnG. The corresponding evaluation metrics, summarized in Tables 3 and 4, demonstrate that **UnifDR** consistently outperforms all competitors in terms of both CRPS and MSD.

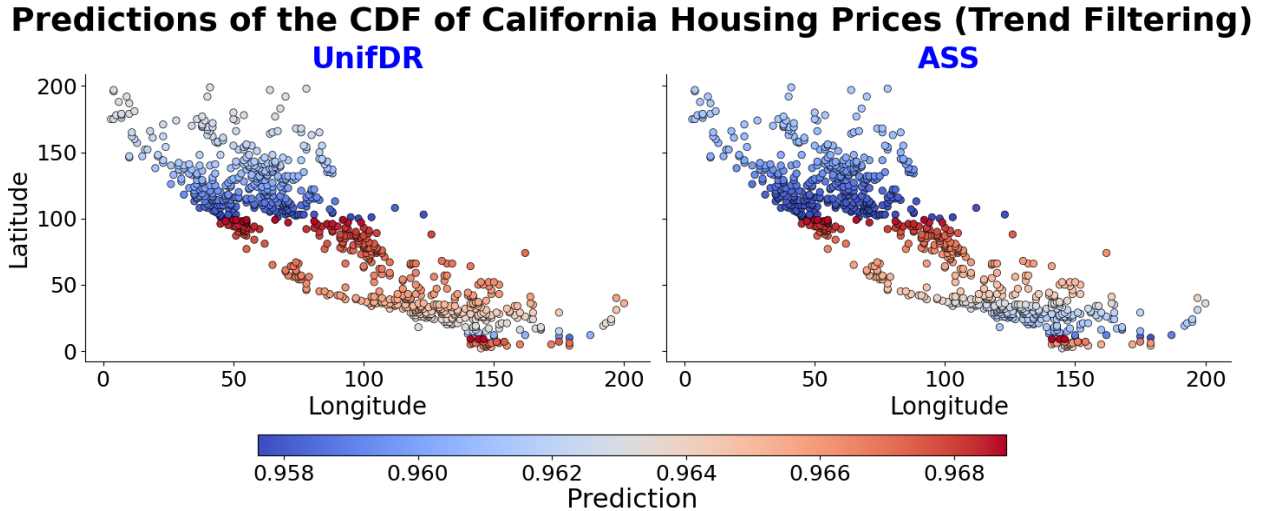


Figure 5: Estimated distribution function $\hat{F}_i(t)$ at $t = 12$ for all grid cells in the test set, comparing UnifDR (Trend Filtering) and the ASS competitor.

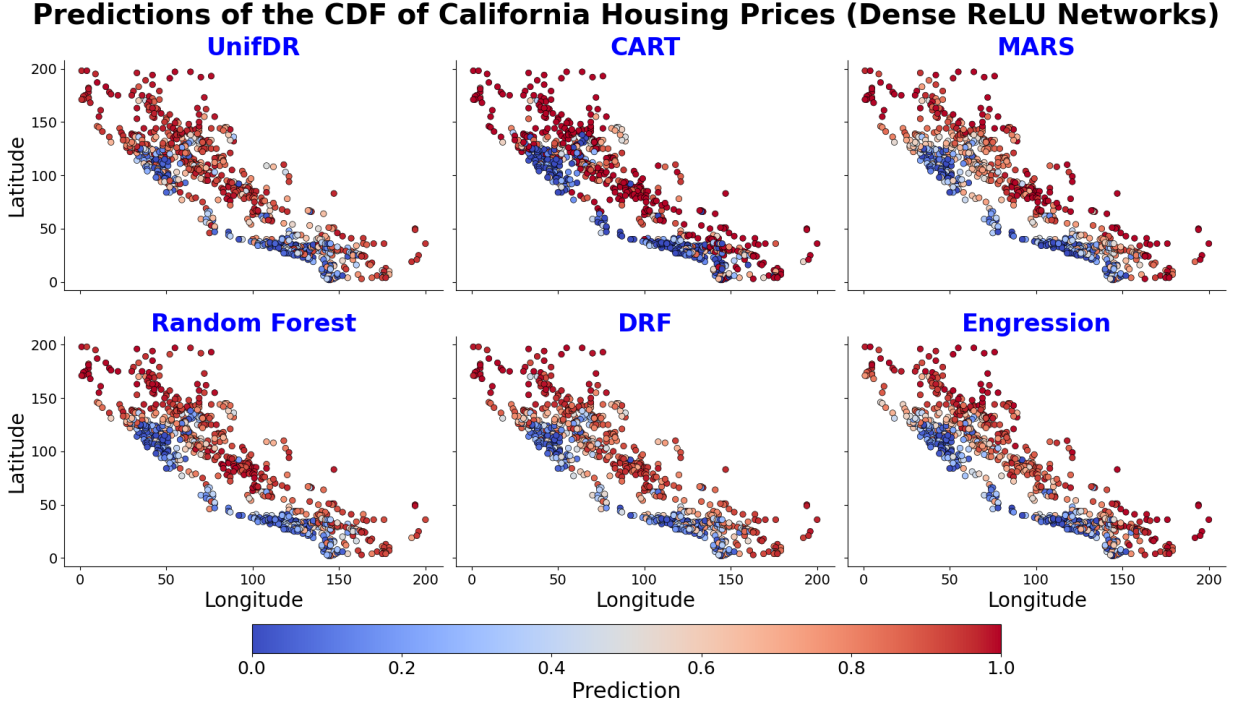


Figure 6: $\hat{F}_i(t)$ for $t = 12$ and all $i \in \text{Test}$, for all competitors.

Table 4: Evaluation metrics for UnifDR (Dense ReLU networks) and its competitors on the California housing price dataset.

METHOD	CRPS (MEAN \pm STD)	MSD (MEAN \pm STD)
UNIFDR	0.0209 \pm 0.00055	0.1450 \pm 0.0047
CART	0.0258 \pm 0.00053	0.1984 \pm 0.0067
DRF	0.0229 \pm 0.00051	0.1755 \pm 0.0045
ENG	0.0244 \pm 0.00059	0.1924 \pm 0.0057
MARS	0.0233 \pm 0.00057	0.1798 \pm 0.0099
RF	0.0221 \pm 0.00046	0.1650 \pm 0.0047

A.1.2 Ozone Data Analysis

We further evaluate the effectiveness of the proposed **UnifDR** method by analyzing ozone concentration data collected from the Environmental Protection Agency (EPA) Regional dataset. This dataset consists of daily ozone measurements collected across various monitoring stations in different regions of the United States for the year 2024. The dataset includes measurements of ozone concentration along with associated variables such as Air Quality Index (AQI), wind speed, temperature, latitude, and longitude. The available variables include: State Code, County Code, Site Number, Latitude, Longitude, Date (Year, Month, Day), Ozone concentration (in parts per million), AQI,

Wind Speed (in miles per hour), Temperature (in Fahrenheit), Observation Percentage (percentage of valid observations for a given day), First Maximum Value (highest ozone level recorded in a day), First Maximum Hour (time at which the maximum value was recorded), and Observation Count (number of valid ozone measurements per day). The data are publicly accessible via the EPA’s AirData portal at https://aqs.epa.gov/aqsweb/airdata/download_files.html, where historical records spanning multiple years can be downloaded.

Following the approach of previous studies, the geographic region of interest is discretized based on latitude and longitude coordinates, specifically within the range $30^{\circ}N$ to $50^{\circ}N$ and $-153^{\circ}W$ to $-70^{\circ}W$. In the Trend Filtering setup, each monitoring site within these bounds is uniquely identified using a lexicographic ordering of its latitude and longitude values. The response variable y_i for each site i is defined as the mean of the daily recorded ozone levels, ensuring robustness against short-term fluctuations and missing data. This approach results in a total of 1,189 unique monitoring sites, which serve as the basis for spatial trend estimation.

In contrast, the Dense ReLU network method allows for a flexible spatial fit by incorporating spatial location data as covariates, capturing complex relationships that influence ozone concentration. Specifically, the model uses latitude, longitude, mean AQI, mean percentage of valid observations, mean 1st maximum ozone value, mean 1st maximum hour, and mean observation count as input features. The Dense ReLU network consists of two hidden layers, each containing 100 neurons followed by a ReLU activation function.

Evaluations are performed over 100 evenly spaced points within the range $[0, 1]$. Figures 7 and 8 present the estimated cumulative distribution functions $\hat{F}_i(t)$ at $t = 0.03$, comparing the performance of **UnifDR** using Trend Filtering and Dense ReLU network against their competitors. Tables 5 and 6 summarize the evaluation metrics, demonstrating that **UnifDR** achieves superior performance in terms of both CRPS and MSD.

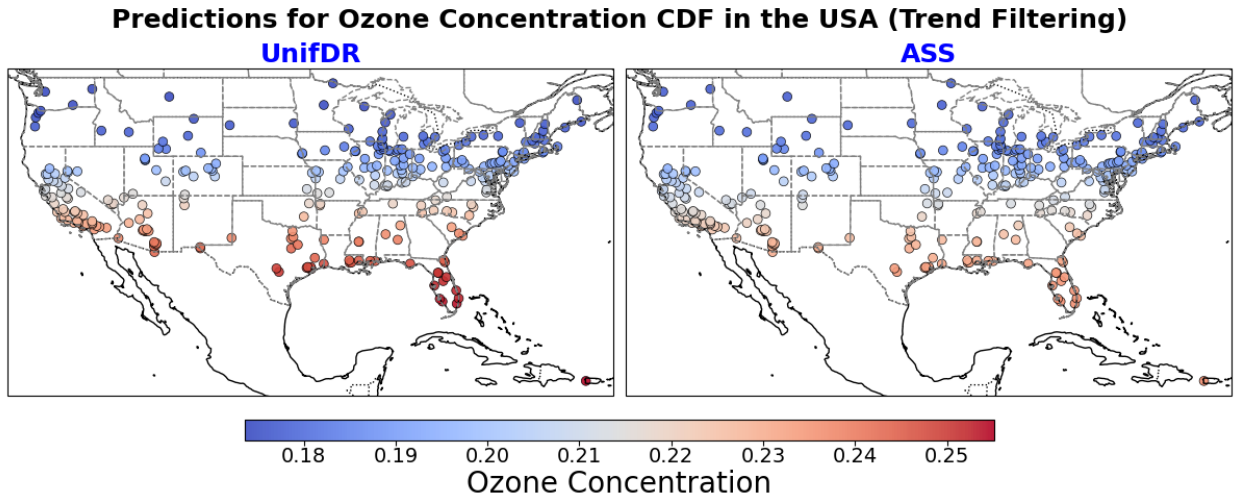


Figure 7: Estimated distribution function $\hat{F}_i(t)$ for all monitoring sites in the test set, comparing UnifDR (Trend Filtering) and the ASS competitor.

Table 5: Evaluation metrics for UnifDR and its competitor ASS on the ozone concentration dataset.

METHOD	CRPS (MEAN ± STD)	MSD (MEAN ± STD)
UNIFDR	0.0027 ± 0.0002	0.1581 ± 0.0124
ASS	0.0035 ± 0.0002	0.1987 ± 0.0127

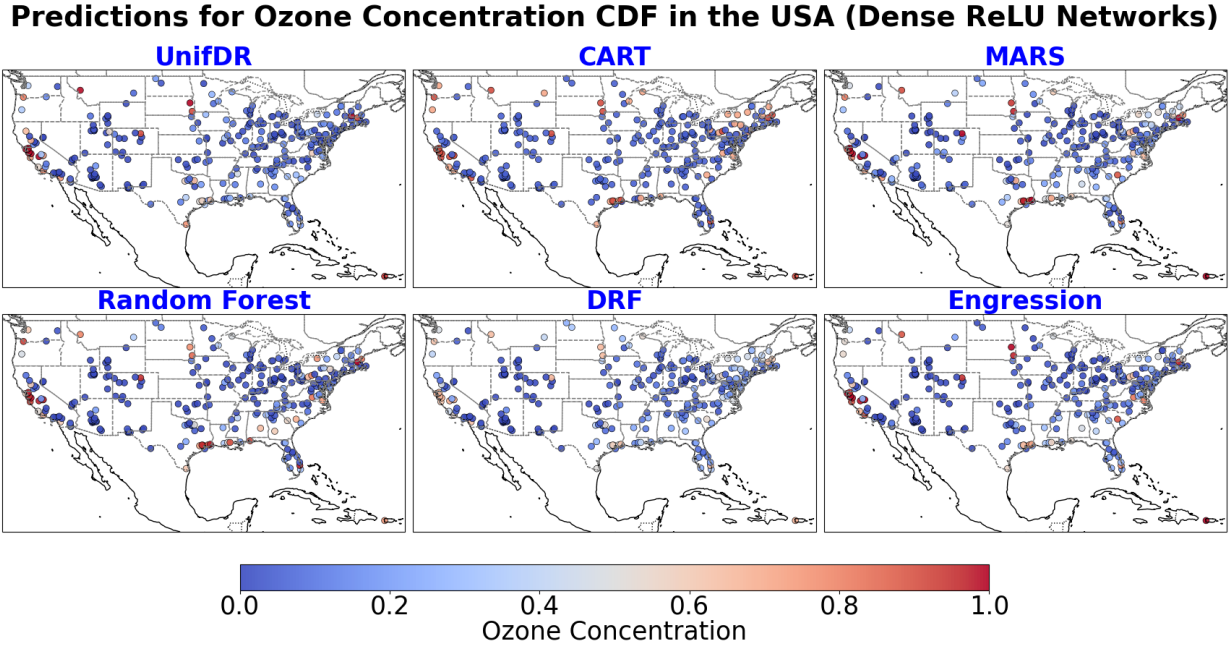


Figure 8: $\hat{F}_i(t)$ for $t = 0.03$ and all $i \in \text{Test}$, for all competitors.

Table 6: Evaluation metrics for UnifDR (Dense ReLU networks) and its competitors on the Ozone dataset.

METHOD	CRPS (MEAN ± STD)	MSD (MEAN ± STD)
UNIFDR	0.0016 ± 0.00021	0.0959 ± 0.0136
CART	0.0026 ± 0.00028	0.1529 ± 0.0209
DRF	0.0031 ± 0.00016	0.1593 ± 0.0118
ENG	0.0022 ± 0.00099	0.1097 ± 0.0603
MARS	0.0022 ± 0.00039	0.1288 ± 0.0376
RF	0.0021 ± 0.00023	0.1012 ± 0.0157

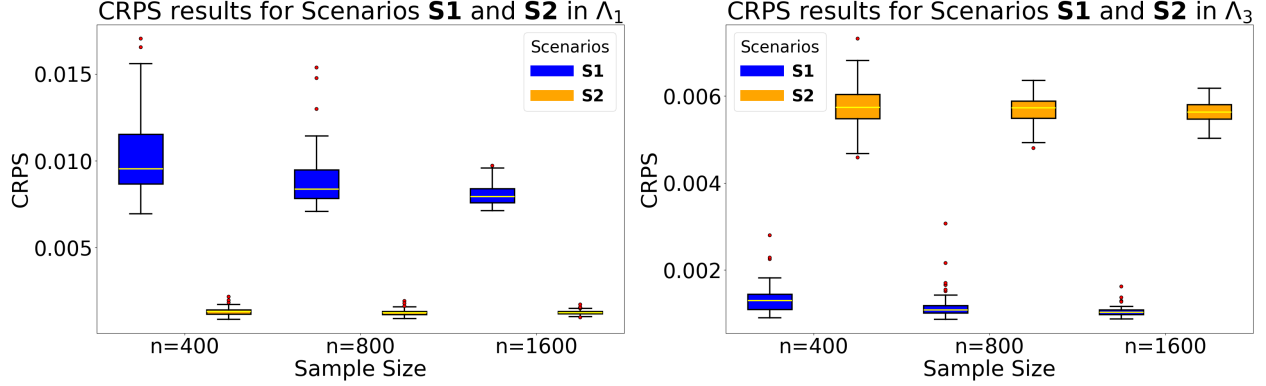


Figure 9: Box plots for simulation results of **S1-S2** for the CRPS metric. The left plot corresponds to Λ_1 , while the right plot corresponds to Λ_3 .

A.2 CRPS results on Test Sets Λ_1 , and Λ_3

Section 4.1 presented evaluation results for the test set Λ_2 using the Continuous Ranked Probability Score (CRPS), where Λ_2 represents a balanced range of values centered around zero. To provide a more comprehensive analysis, this appendix reports the CRPS results for the alternative test sets Λ_1 and Λ_3 , which emphasize distinct distributional regions.

The test sets are defined as follows:

- Λ_1 : 100 points evenly spaced between -1 and 0.4 , focusing on the lower and middle ranges of the distribution.
- Λ_3 : 100 points evenly spaced between 0.8 and 10 , capturing the upper tail of the distribution.

This extended analysis provides deeper insights into the robustness of the proposed methods in varying distributional regimes, including regions with lower densities and heavier tails. As described in Section 4.1, for each test set (Λ_1 , and Λ_3), the CRPS is computed and averaged over 100 Monte Carlo repetitions. Figures 9 through 13 summarize the CRPS results across different scenarios and evaluation regions. Specifically, Figure 9 correspond to Scenarios **S1** and **S2** in Λ_1 and Λ_3 . Figure 10 present Scenarios **S3** and **S4** in Λ_1 and Λ_3 . Figure 11 focuses on Scenario **S5** in Λ_1 and Λ_3 . Figures 12 and 13 consider Scenario **S6** in Λ_1 and Λ_3 .

Across all scenarios, **UnifDR** is implemented using different estimation methods: the isotonic estimator for **S1** and **S2** (Section 2.3), the trend filtering estimator for **S3** and **S4** (Section 2.4), and the Dense ReLU Networks method for **S5** and **S6** (Section 3.2). Our proposed framework **UnifDR** outperforms competing approaches across all scenarios, evaluation regions, and sample sizes, regardless of the specific estimation method employed. These findings highlight the versatility and robustness of **UnifDR** in adapting to diverse structural patterns within the data. Overall, performance trends remain consistent across Λ_1 , Λ_2 , and Λ_3 , with minor variations due to differences in the underlying data distributions. This extended analysis further reinforces the effectiveness of the proposed methods under varying test conditions.

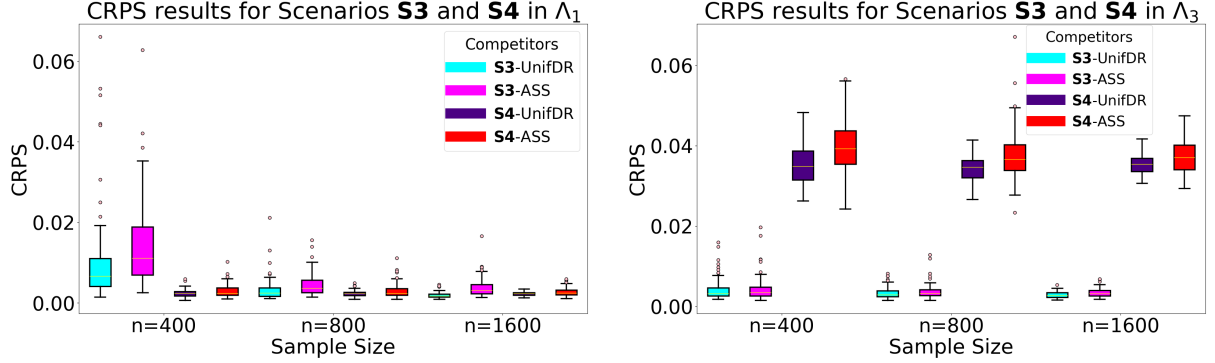


Figure 10: Box plots for simulation results of **S3-S4** for the CRPS metric. The row shows results for Λ_1 (left) and Λ_3 (right).

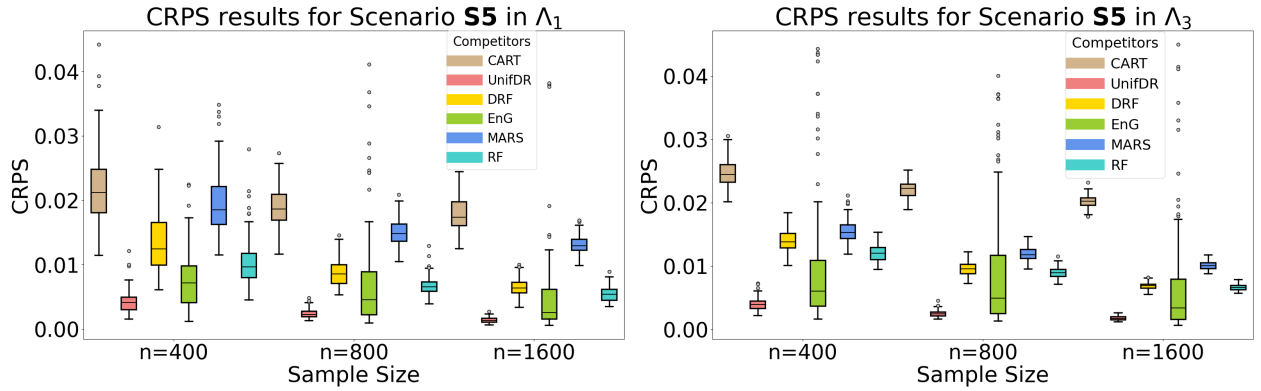


Figure 11: Box plots for simulation results of **S5** for the CRPS metric. The row shows results for Λ_1 (left) and Λ_3 (right).

A.3 Additional Results for Maximum Squared Difference (MSD) Metric

This appendix extends the results presented in Section 4.1 and Appendix A.2 by providing evaluations of the Maximum Squared Difference (MSD) metric across all scenarios for the test sets Λ_1 , Λ_2 , and Λ_3 . The MSD metric measures the worst-case discrepancy between the estimated and true cumulative distribution functions (CDFs), offering a stringent assessment of model accuracy and robustness.

Figure 14 displays box plots of the MSD results for Scenarios **S1** and **S2** across all test sets. As outlined in Section 4.1, **UnifDR** employs isotonic regression for these scenarios, which lacks direct competitors. The results indicate a decreasing trend in MSD values as the sample size increases, demonstrating the consistency and improved accuracy of isotonic regression with larger datasets. Moreover, variations in MSD across Λ_1 , Λ_2 , and Λ_3 reflect natural differences in the underlying data distributions.

Figure 15 presents MSD results for Scenarios **S3** and **S4**, where **UnifDR** employs trend filtering and is compared against the additive smoothing splines (ASS) method. Across all test sets and sample sizes, **UnifDR** consistently outperforms ASS, demonstrating its ability to adapt to complex

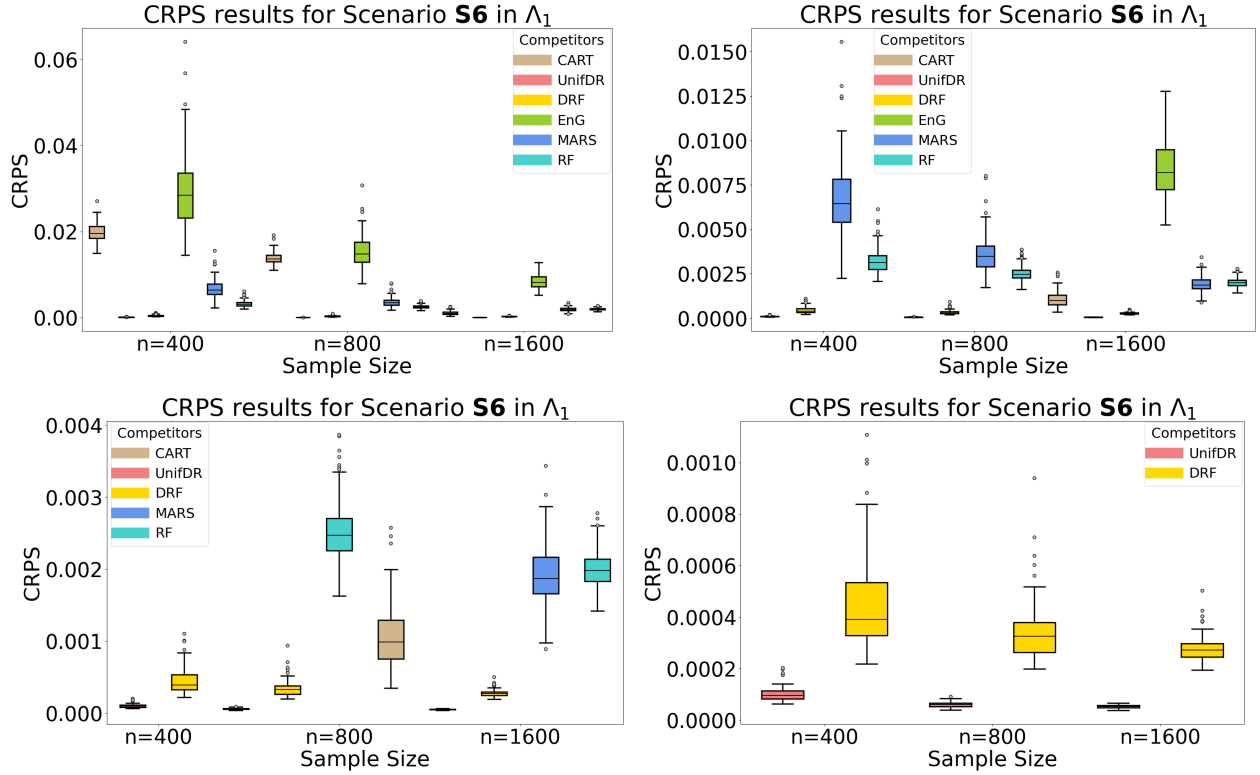


Figure 12: Box plots for simulation results of **S6** for the CRPS metric for the set Λ_1 . The top row shows results for the all the competitors (left) and, competitors with median below 0.01 (right). The bottom row displays results for competitors with median below 0.0025 (left), and best two competitors (right).

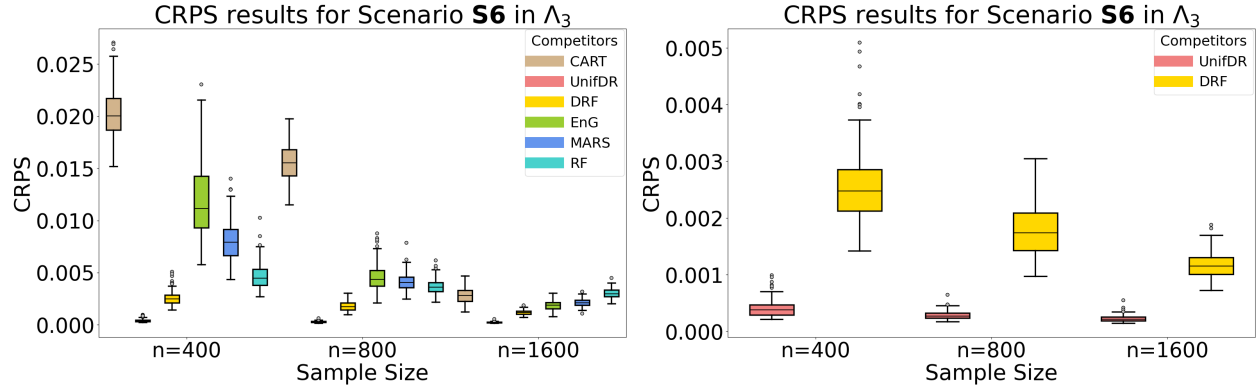


Figure 13: Box plots for simulation results of **S6** for the CRPS metric using evaluation set Λ_3 . The left plot corresponds to all competitors performance, while the right plot corresponds to best two competitors.

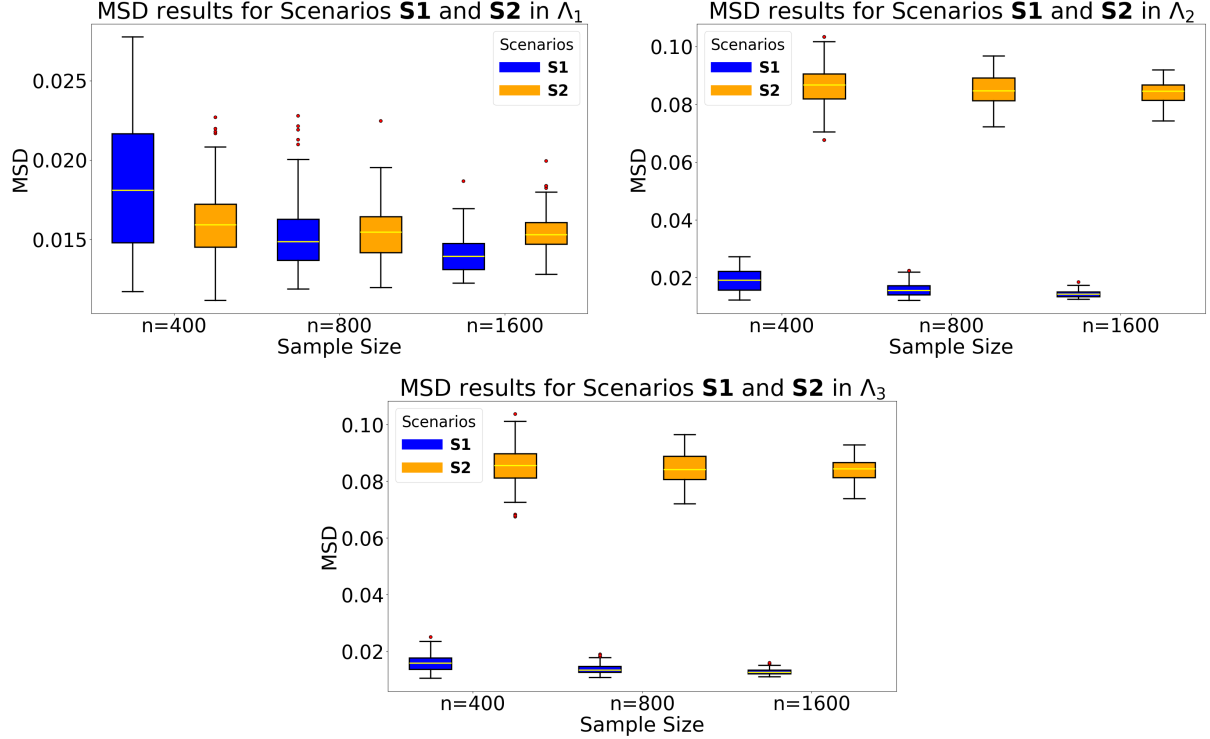


Figure 14: Box plots for MSD results in Scenarios **S1** and **S2**. The top row shows results for Λ_1 (left) and Λ_2 (right), while the bottom row displays results for Λ_3 .

structural variations. Notably, trend filtering exhibits particularly strong performance in regions with sparse or heavy-tailed data distributions.

Figures 16 to 19 summarize MSD results for Scenarios **S5** and **S6**, where **UnifDR** is implemented via Dense ReLU Networks (Section 3.2). The results further confirm the superiority of **UnifDR** over all competing methods, maintaining its advantage across different sample sizes and evaluation sets. As observed with the CRPS metric, **UnifDR** effectively captures diverse structural patterns and remains robust in challenging scenarios involving data sparsity and heavy tails.

The inclusion of MSD results provides a comprehensive performance evaluation of **UnifDR**, reinforcing its effectiveness and reliability across various experimental conditions.

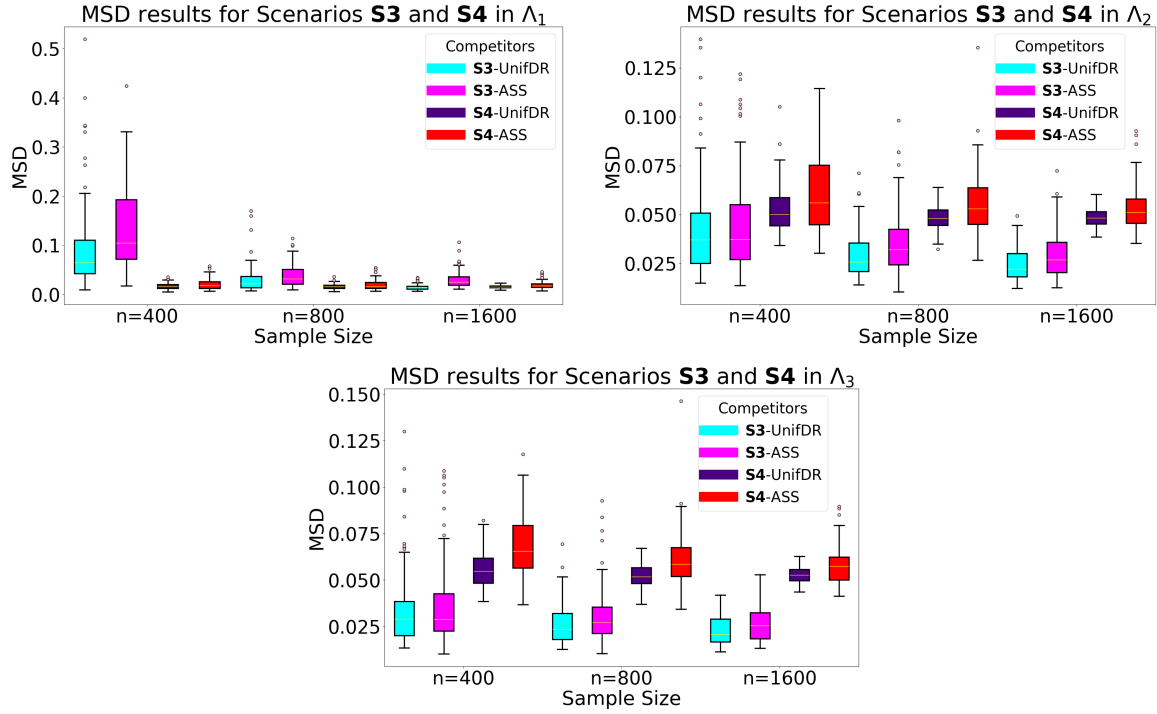


Figure 15: Box plots for MSD in **S3** and **S4**. The top row shows results for Λ_1 (left) and Λ_2 (right), while the bottom row displays results for Λ_3 .

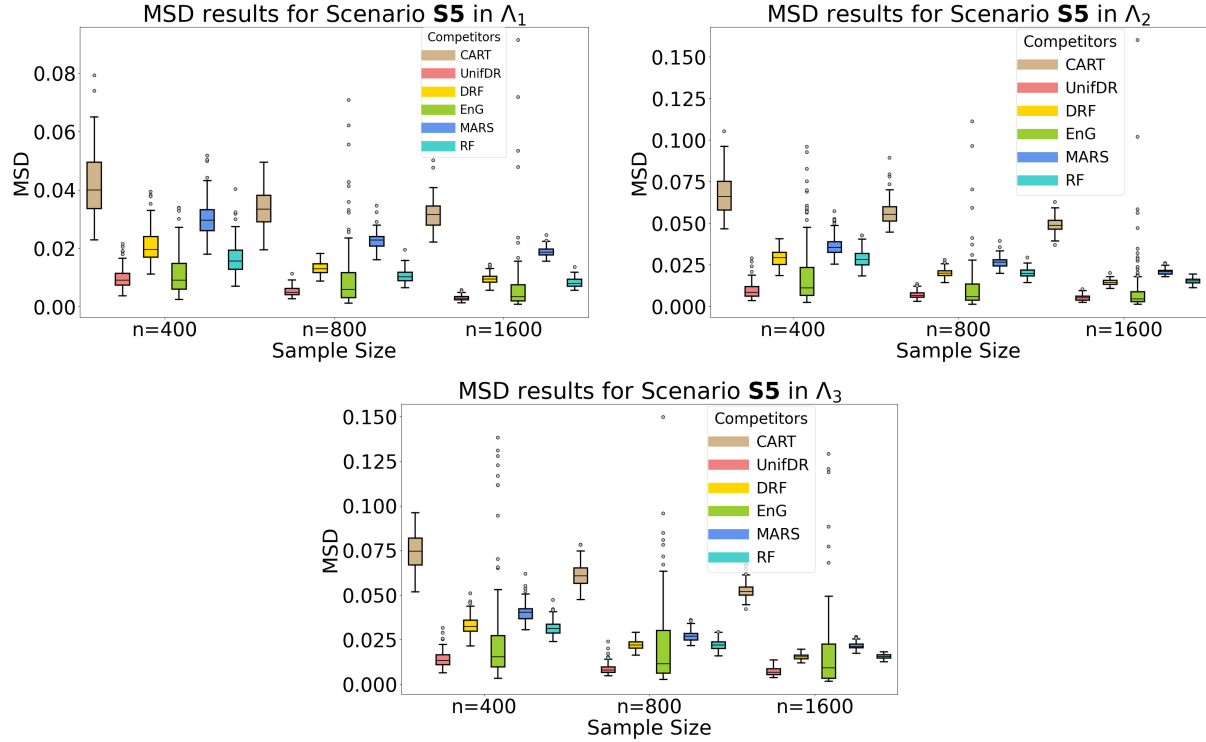


Figure 16: Box plots for MSD in **S5**. The top row shows results for Λ_1 (left) and Λ_2 (right), while the bottom row displays results for Λ_3 .

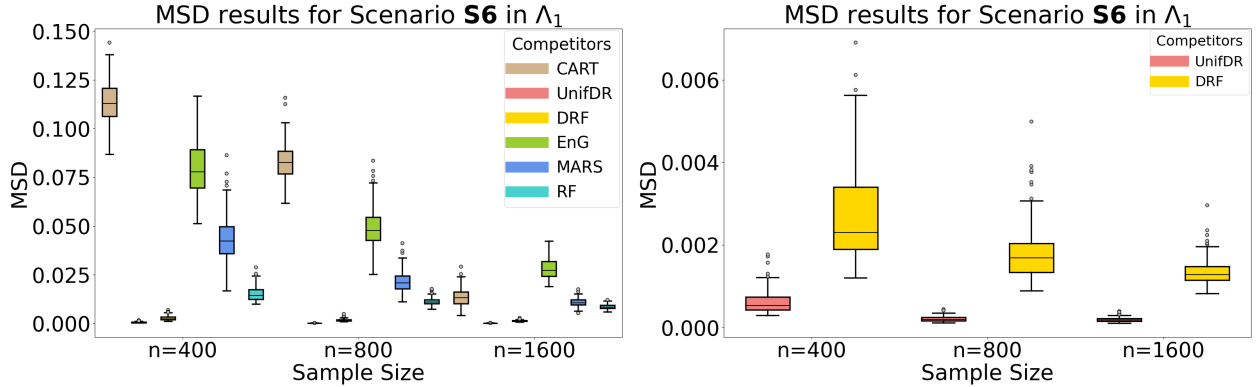


Figure 17: Box plots for MSD in **S6** using evaluation set Λ_1 . The left plot corresponds to all competitors performance, while the right plot corresponds to best two competitors.

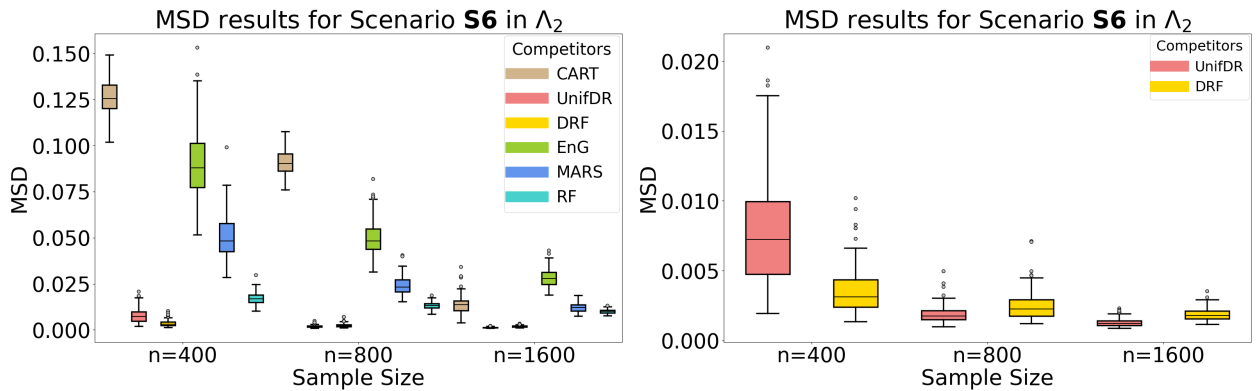


Figure 18: Box plots for MSD in **S6** using evaluation set Λ_2 . The left plot corresponds to all competitors performance, while the right plot corresponds to best two competitors.

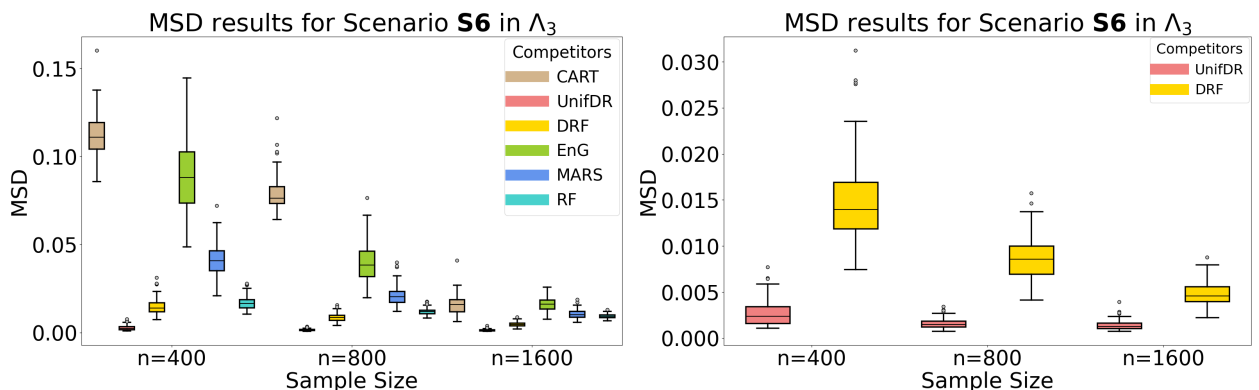


Figure 19: Box plots for MSD in **S6** using evaluation set Λ_3 . The left plot corresponds to all competitors performance, while the right plot corresponds to best two competitors.

A Proofs

B Proof of Lemma 1

Proof. Let $y_{(1)} \leq y_{(2)} \leq \dots \leq y_{(n)}$ the order statistics of y . Notice that

$$\begin{aligned} L(F) &:= \sum_{i=1}^n \text{CRPS}(F_i, 1\{y_i \leq \cdot\}) \\ &= \int \sum_{i=1}^n (F_i(t) - 1\{y_i \leq t\})^2 dt \\ &= \sum_{j=1}^{n+1} \int_{A_j} \sum_{i=1}^n (F_i(t) - 1\{y_i \leq t\})^2 dt \end{aligned}$$

where $A_1 = (-\infty, y_{(1)})$, $A_2 = [y_{(1)}, y_{(2)})$, \dots , $A_n = [y_{(n-1)}, y_{(n)})$, $A_{n+1} = [y_{(n)}, \infty)$. However, for every $j \in \{1, \dots, n+1\}$ and $t, t' \in A_j$ we have that

$$\min_{F(t) \in K} \sum_{i=1}^n (F_i(t) - 1\{y_i \leq t\})^2 = \min_{F(t') \in K} \sum_{l=1}^n (F_l(t') - 1\{y_l \leq t'\})^2.$$

Hence, letting t_j be an element of A_j , we obtain that minimizing $L(F)$ with the constraints $F(t) \in K$ for all t is equivalent to solving the independent problems

$$\min_{F(t_j) \in K} \sum_{i=1}^n (F_i(t_j) - 1\{y_i \leq t_j\})^2,$$

and the claim follows. \square

B.1 Proof of Theorem 1

Theorem 8. [*Theorem A.1 in Guntuboyina et al. (2020)*]. *There exists a universal positive constant $C > 0$ such that for every t ,*

$$\frac{1}{n} \mathbb{E} \left(\sum_{i=1}^n (\widehat{F}_i(t) - F_i^*(t))^2 \right) \leq \frac{C \max\{\eta^2, \max_{i=1,\dots,n} F_i^*(t)(1 - F_i^*(t))\}}{n},$$

for every $\eta > 1$ satisfying

$$\mathbb{E} \left[\sup_{\theta \in K_t : \|\theta - F^*(t)\| \leq \eta} \epsilon(t)^\top (\theta - F^*(t)) \right] \leq \frac{\eta^2}{2} \quad (23)$$

where $\epsilon(t) = w(t) - F^*(t)$.

In the followig we first present the proof of Theorem 8.

Proof. Let $t \in \mathbb{R}$. Define $\sigma^2 = \max_{i=1,\dots,n} F_i^*(t)(1 - F_i^*(t))$. We consider the following two cases separately based on the value of σ :

1. $\sigma = 0$,

2. $\sigma \neq 0$.

Case 1: $\sigma = 0$.

By definition, $\sigma^2 = \max_{i=1,\dots,n} F_i^*(t)(1 - F_i^*(t)) = 0$. This implies that for all $i = 1, \dots, n$, $F_i^*(t)(1 - F_i^*(t)) = 0$. Since $F_i^*(t)(1 - F_i^*(t)) = 0$, it follows that either $F_i^*(t) = 0$ or $F_i^*(t) = 1$ for each i . Now observe that for each $i \in \{1, \dots, n\}$, either $w_i(t) = 0$ or $w_i(t) = 1$. Given that $\mathbb{E}(w_i(t)) = F_i^*(t)$, it follows that $w_i(t) = F_i^*(t)$. Therefore, by the definition of \widehat{F} in Equation 1, we have $\widehat{F} = F^*$. In this case, it holds that

$$\mathbb{E} \left(\|\widehat{F}(t) - F^*(t)\|_2^2 \right) = 0,$$

and the result is obtained trivially.

Case 2: $\sigma \neq 0$.

Denote by $\Theta_{F^*(t)}(\eta) := \{\theta - F^*(t) \in \Theta_{F^*(t)} : \|\theta - F^*(t)\|_2 \leq \eta\}$, where $\Theta_{F^*(t)} = \{\theta - F^*(t) : \theta \in K_t\}$. Notice that the function $L : \mathbb{R}^n \rightarrow \mathbb{R}$ given by

$$\epsilon \rightarrow \sup_{\theta \in \Theta_{F^*(t)}(\eta)} \left| \epsilon^\top (\theta - F^*(t)) \right|$$

is η -Lipschitz. Moreover observe that L is separately convex. In fact, for any $k \in \{1, \dots, n\}$ we have that

$$\begin{aligned} & (\epsilon_1, \dots, \epsilon_{k-1}, t\epsilon_k^{(1)} + (1-t)\epsilon_k^{(2)}, \epsilon_{k+1}, \dots, \epsilon_n) \\ &= (t\epsilon_1, \dots, t\epsilon_{k-1}, t\epsilon_k^{(1)}, t\epsilon_{k+1}, \dots, t\epsilon_n) \\ &+ ((1-t)\epsilon_1, \dots, (1-t)\epsilon_{k-1}, (1-t)\epsilon_k^{(2)}, (1-t)\epsilon_{k+1}, \dots, (1-t)\epsilon_n) \\ &= t\epsilon_{k,1} + (1-t)\epsilon_{k,2}. \end{aligned}$$

Therefore,

$$\begin{aligned} & L \left[(\epsilon_1, \dots, \epsilon_{k-1}, t\epsilon_k^{(1)} + (1-t)\epsilon_k^{(2)}, \epsilon_{k+1}, \dots, \epsilon_n) \right] \\ &= \sup_{\theta \in \Theta_{F^*(t)}(\eta)} \left| (t\epsilon_{k,1} + (1-t)\epsilon_{k,2})^\top (\theta - F^*(t)) \right| \\ &= \sup_{\theta \in \Theta_{F^*(t)}(\eta)} \left| t(\epsilon_{k,1})^\top (\theta - F^*(t)) + (1-t)(\epsilon_{k,2})^\top (\theta - F^*(t)) \right| \\ &\leq \sup_{\theta \in \Theta_{F^*(t)}(\eta)} \left[t \left| (\epsilon_{k,1})^\top (\theta - F^*(t)) \right| + (1-t) \left| (\epsilon_{k,2})^\top (\theta - F^*(t)) \right| \right], \end{aligned}$$

where the inequality is followed by triangle inequality. Using the fact that the supremum of the sum is bounded by the sum of the supremums, it follows that

$$\begin{aligned} & L \left[(\epsilon_1, \dots, \epsilon_{k-1}, t\epsilon_k^{(1)} + (1-t)\epsilon_k^{(2)}, \epsilon_{k+1}, \dots, \epsilon_n) \right] \\ &\leq t \sup_{\theta \in \Theta_{F^*(t)}(\eta)} \left| (\epsilon_{k,1})^\top (\theta - F^*(t)) \right| + (1-t) \sup_{\theta \in \Theta_{F^*(t)}(\eta)} \left| (\epsilon_{k,2})^\top (\theta - F^*(t)) \right| \\ &= tL \left[(\epsilon_1, \dots, \epsilon_{k-1}, \epsilon_k^{(1)}, \epsilon_{k+1}, \dots, \epsilon_n) \right] + (1-t)L \left[(\epsilon_1, \dots, \epsilon_{k-1}, \epsilon_k^{(2)}, \epsilon_{k+1}, \epsilon_n) \right]. \end{aligned}$$

Thus, L is separately convex. Notice that $\epsilon_i(t) = (1\{y_i \leq t\} - F_i^*(t))$ satisfies $|\epsilon_i(t)| \leq 1$. Hence, by Theorem 3.4 in [Wainwright \(2019\)](#), for any $\delta > 0$

$$\sup_{\theta \in \Theta_{F^*(t)}(\eta)} |\epsilon(t)^\top (\theta - F^*(t))| \leq \mathbb{E} \left(\sup_{\theta \in \Theta_{F^*(t)}(\eta)} |\epsilon(t)^\top (\theta - F^*(t))| \right) + \sigma\eta\delta \quad (24)$$

with probability at least $1 - e^{-\delta^2\sigma^2/16}$. Next, we have that

$$|\epsilon(t)^\top (\theta - F^*(t))| \leq \max\left\{\frac{\|\theta - F^*(t)\|_2}{\eta}, 1\right\} \tilde{L}(\eta), \quad (25)$$

for any $\theta \in K_t$, where $\tilde{L}(\eta) = \sup_{\theta \in \Theta_{F^*(t)}(\eta)} |\epsilon(t)^\top (\theta - F^*(t))|$. This conclusion is derived based on the subsequent line of reasoning. If $\theta \in K_t$ and $\|\theta - F^*(t)\|_2 \leq \eta$, then $\theta - F^*(t) \in \Theta_{F^*(t)}(\eta)$ and in consequence $|\epsilon(t)^\top (\theta - F^*(t))| \leq \tilde{L}(\eta)$, by definition of $\tilde{L}(\eta)$. If $\theta \in K_t$ and $\|\theta - F^*(t)\|_2 > \eta$, then $\frac{\theta - F^*(t)}{\|\theta - F^*(t)\|_2} \cdot \eta \in \Theta_{F^*(t)}(\eta)$ because $\Theta_{F^*(t)}$ is star-shaped, given that K_t is convex. Also $\left\| \frac{\theta - F^*(t)}{\|\theta - F^*(t)\|_2} \eta \right\|_2 = \eta$. Hence,

$$\left| \epsilon(t)^\top \left(\frac{\theta - F^*(t)}{\|\theta - F^*(t)\|_2} \eta \right) \right| \leq \tilde{L}(\eta),$$

which implies,

$$|\epsilon(t)^\top (\theta - F^*(t))| \leq \frac{\|\theta - F^*(t)\|_2}{\eta} \cdot \tilde{L}(\eta),$$

for any $\theta \in K_n$. Then we observe that by the basic inequality

$$\|w(t) - \hat{F}(t)\|_2^2 \leq \|w(t) - F^*(t)\|_2^2.$$

This implies that

$$\frac{1}{2} \|\hat{F}(t) - F^*(t)\|_2^2 \leq \epsilon(t)^\top (\hat{F}(t) - F^*(t)).$$

Given that $\hat{F}(t) \in K_t$ it follows from inequality (25) that

$$\frac{1}{2} \|\hat{F}(t) - F^*(t)\|_2^2 \leq \max\left\{\frac{\|\hat{F}(t) - F^*(t)\|_2}{\eta}, 1\right\} \tilde{L}(\eta),$$

and by inequality (24),

$$\frac{1}{2} \|\hat{F}(t) - F^*(t)\|_2^2 \leq \max\left\{\frac{\|\hat{F}(t) - F^*(t)\|_2}{\eta}, 1\right\} \left(\mathbb{E} \left(\sup_{\theta \in \Theta_{F^*(t)}(\eta)} |\epsilon(t)^\top (\theta - F^*(t))| \right) + \sigma\eta\delta \right),$$

for any $\delta > 0$, with probability at least $1 - e^{-\sigma^2\delta^2/16}$. Thus, for any $\delta > 0$

$$\|\hat{F}(t) - F^*(t)\|_2 \leq \max \left\{ \frac{2G(\eta, \delta)}{\eta}, \sqrt{2G(\eta, \delta)} \right\},$$

with probability at least $1 - e^{-\sigma^2 \delta^2 / 16}$, where $G(\eta, \delta) = \mathbb{E} \left(\sup_{\theta \in \Theta_{F^*(t)}(\eta)} |\epsilon(t)^\top (\theta - F^*(t))| \right) + \sigma \eta \delta$. Next, by inequality (23),

$$\max \left\{ \frac{2G(\eta, \delta)}{\eta} \sqrt{2G(\eta, \delta)} \right\} \leq \max \left\{ \frac{\eta^2 + 2\sigma\eta\delta}{\eta}, \sqrt{\eta^2 + 2\sigma\eta\delta} \right\} = \max \left\{ \eta + 2\sigma\delta, \sqrt{\eta(\eta + 2\sigma\delta)} \right\} \leq \eta + 2\sigma\delta.$$

In consequence for any $\delta > 0$,

$$\|\widehat{F}(t) - F^*(t)\|_2 \leq \eta + 2\sigma\delta, \quad (26)$$

with probability at least $1 - e^{-\sigma^2 \delta^2 / 16}$. Finally, we observe that

$$\begin{aligned} \mathbb{E}(\|\widehat{F}(t) - F^*(t)\|_2^2) &= \int_0^\infty \mathbb{P} \left(\|\widehat{F}(t) - F^*(t)\|_2^2 > s \right) ds \\ &= \int_0^{(\eta+2\sigma)^2} \mathbb{P} \left(\|\widehat{F}(t) - F^*(t)\|_2^2 > s \right) ds + \int_{(\eta+2\sigma)^2}^\infty \mathbb{P} \left(\|\widehat{F}(t) - F^*(t)\|_2^2 > s \right) ds \\ &= I_1 + I_2. \end{aligned}$$

To analyze the term I_1 we observe that $\mathbb{P} \left(\|\widehat{F}(t) - F^*(t)\|_2^2 > s \right) \leq 1$, and therefore

$$I_1 \leq (\eta + 2\sigma)^2. \quad (27)$$

For the term I_2 , we perform a change of variables $s = (\eta + 2\sigma\delta)^2$ to obtain

$$I_2 \leq \int_1^\infty \mathbb{P} \left(\|\widehat{F}(t) - F^*(t)\|_2^2 > (\eta + 2\sigma\delta)^2 \right) 4\sigma(\eta + 2\sigma\delta)d\delta,$$

and by inequality (26),

$$I_2 \leq 4\sigma \int_1^\infty e^{-\frac{\sigma^2 \delta^2}{16}} (\eta + 2\sigma\delta)d\delta. \quad (28)$$

Moreover,

$$\begin{aligned} 4\sigma \int_1^\infty e^{-\frac{\sigma^2 \delta^2}{16}} (\eta + 2\sigma\delta)d\delta &= 4\eta\sigma \int_1^\infty e^{-\frac{\sigma^2 \delta^2}{16}} d\delta + 8\sigma^2 \int_1^\infty e^{-\frac{\sigma^2 \delta^2}{16}} \delta d\delta \\ &= 2\eta \frac{\sqrt{\pi}\sigma \operatorname{erfc}(\sigma)}{\sigma} + 4e^{-\sigma^2} \\ &\leq 2\eta\sqrt{\pi} \operatorname{erfc}(\sigma) + 4e^{-\sigma^2}. \end{aligned}$$

where $\operatorname{erfc}(z) = \frac{2}{\sqrt{\pi}} \int_z^\infty e^{-\delta^2} d\delta$. From inequality (27) (28), and the fact that $\eta > 1$, we conclude that

$$\mathbb{E}(\|\widehat{F}(t) - F^*(t)\|_2^2) \leq C_1(\eta^2 + \sigma^2),$$

for an absolute positive constant C_1 . Finally observe that,

$$\eta^2 + \sigma^2 \leq 2 \max(\eta^2, \sigma^2)$$

Taking $C = 2C_1$ the result is achieved. \square

Now we are ready to start the proof of Theorem 1.

Proof. Notice that for all i , it holds that $\widehat{F}_i(t) = F^*(t) = 0$ for all $t < \inf\{a : a \in \Omega\}$ and $\widehat{F}_i(t) = F^*(t) = 1$ for all $t > \sup\{a : a \in \Omega\}$. Hence,

$$\begin{aligned} \mathbb{E} \left(\frac{1}{n} \sum_{i=1}^n \text{CRPS}(\widehat{F}_i, F_i^*) \right) &= \mathbb{E} \left(\frac{1}{n} \sum_{i=1}^n \int_{-\infty}^{\infty} (\widehat{F}_i(t) - F_i^*(t))^2 dt \right) \\ &= \mathbb{E} \left(\frac{1}{n} \sum_{i=1}^n \int_{\Omega} (\widehat{F}_i(t) - F_i^*(t))^2 dt \right) \\ &= \int_{\Omega} \mathbb{E} \left(\frac{1}{n} \sum_{i=1}^n (\widehat{F}_i(t) - F_i^*(t))^2 \right) dt \\ &\leq \int_{\Omega} \frac{C \max\{1, \eta^2\}}{n} dt \\ &= \frac{C \max\{1, \eta^2\}}{n} \int_{\Omega} dt \end{aligned}$$

where the inequality follows from Theorem 8, by noticing that (4) and Lemma 4 imply (23). \square

B.2 Proof of Corollary 1

Throughout we use the notation from Definitions 5 and 6.

First, notice that $\widehat{F}_i(t) = \widetilde{F}_i(t) = 0$ for all $t < y_{(1)}$ and for all i . Similarly, $\widehat{F}_i(t) = \widetilde{F}_i(t) = 1$ for all $t \geq y_{(n)}$ and for all i . Therefore,

$$\int_{-\infty}^{y_{(1)}} (\widehat{F}_i^+(t) - F_i^*(t))^2 + \int_{y_{(n)}}^{\infty} (\widehat{F}_i^+(t) - F_i^*(t))^2 = \int_{-\infty}^{y_{(1)}} (\widetilde{F}_i(t) - F_i^*(t))^2 + \int_{y_{(n)}}^{\infty} (\widetilde{F}_i(t) - F_i^*(t))^2. \quad (29)$$

Next, define

$$\widehat{G}_i(t) := \begin{cases} \widehat{F}_i^+((1-t)(y_{(n)} - y_{(1)}) + y_{(1)}) & \text{for } t \in [0, 1], \\ 0 & \text{otherwise.} \end{cases}$$

Clearly, $\widehat{G}_i(0) = \widehat{F}_i^+(y_{(n)})$ and $\widehat{G}_i(1) = \widehat{F}_i^+(y_{(1)})$. Moreover, recalling that for $t \in [y_{(1)}, y_{(n)}]$, we can write

$$\widehat{F}_i^+(t) = \sum_{k=1}^{n-1} a_{i,j_k} 1_{[y_{(j_k)}, y_{(j_k+1)})}(t),$$

then for $t \in [0, 1]$, it holds that

$$\widehat{G}_i(t) := \sum_{k=1}^{n-1} a_{i,j_k} 1_{[u_{j_k+1}, u_{j_k})}(t) \quad (30)$$

where

$$u_l := 1 - \frac{y_{(l)} - y_{(1)}}{y_{(n)} - y_{(1)}}$$

for $l \in \{1, \dots, n\}$.

Furthermore, let

$$G_i^*(t) := \begin{cases} F_i^*((1-t)(y_{(n)} - y_{(1)}) + y_{(1)}) & \text{if } t \in [0, 1), \\ 0 & \text{otherwise.} \end{cases}$$

Now, we observe that

$$\begin{aligned} & \int_0^1 (\widehat{G}_i(t) - G_i^*(t))^2 dt \\ &= \int_0^1 (\widehat{F}_i^+((1-t)(y_{(n)} - y_{(1)}) + y_{(1)}) - F_i^*((1-t)(y_{(n)} - y_{(1)}) + y_{(1)}))^2 dt \\ &= \frac{1}{y_{(n)} - y_{(1)}} \int_{y_{(1)}}^{y_{(n)}} (\widehat{F}_i^+(s) - F_i^*(s))^2 ds \end{aligned} \tag{31}$$

by making the change of variable $s = (1-t)(y_{(n)} - y_{(1)}) + y_{(1)}$.

Furthermore, by Lemma 6,

$$\begin{aligned} \int_0^1 |D(G_i^*)(t)|^2 dt &= \int_0^\infty |D(G_i^*)(t)|^2 dt \\ &= \int_0^\infty |G_i^*(t)|^2 dt = \int_0^1 |G_i^*(t)|^2 dt = \frac{1}{y_{(n)} - y_{(1)}} \int_{y_{(1)}}^{y_{(n)}} |F_i^*(s)|^2 ds, \end{aligned} \tag{32}$$

and

$$\begin{aligned} \int_0^1 |D(\widehat{G}_i)(t)|^2 dt &= \int_0^\infty |D(\widehat{G}_i)(t)|^2 dt = \int_0^\infty |\widehat{G}_i(t)|^2 dt \\ &= \int_0^1 |\widehat{G}_i(t)|^2 dt = \frac{1}{y_{(n)} - y_{(1)}} \int_{y_{(1)}}^{y_{(n)}} |\widehat{F}_i^+(s)|^2 ds, \end{aligned} \tag{33}$$

Also, by Lemma 6,

$$\begin{aligned} - \int_0^1 D(\widehat{G}_i)(t) \cdot D(G_i^*)(t) dt &= - \int_0^\infty D(\widehat{G}_i)(t) \cdot D(G_i^*)(t) dt \\ &\leq - \int_0^\infty \widehat{G}_i(t) \cdot G_i^*(t) dt = - \int_0^1 \widehat{G}_i(t) \cdot G_i^*(t) dt \end{aligned} \tag{34}$$

which implies

$$- \int_0^1 D(\widehat{G}_i)(t) \cdot D(G_i^*)(t) dt \leq \frac{1}{y_{(n)} - y_{(1)}} \int_{y_{(1)}}^{y_{(n)}} \widehat{F}_i^+(t) \cdot F_i^*(t) dt. \tag{35}$$

Combining (32), (33) and (34), we obtain that

$$\int_0^1 (D(\widehat{G}_i)(t) - D(G_i^*)(t))^2 dt \leq \frac{1}{y_{(n)} - y_{(1)}} \int_{y_{(1)}}^{y_{(n)}} (\widehat{F}_i^+(t) - F_i^*(t))^2 dt. \tag{36}$$

However, since G_i^* is decreasing and continuous in $[0, 1)$, then by Lemma 6, it holds that $D(G_i^*)(t) = G_i^*(t)$ for all $t \geq 0$. Thus, from (36),

$$\int_0^1 (D(\widehat{G}_i)(t) - G_i^*(t))^2 dt \leq \frac{1}{y_{(n)} - y_{(1)}} \int_{y_{(1)}}^{y_{(n)}} (\widehat{F}_i^+(t) - F_i^*(t))^2 dt. \quad (37)$$

Now, by Lemma 5 and (30), we obtain that

$$D(\widehat{G}_i)(t) := \sum_{l=1}^{n-1} a_{i,j_l} 1_{[m_{l-1}, m_l)}(t) \quad (38)$$

where

$$m_l := \sum_{k=1}^l \frac{y_{(j_k+1)} - y_{(j_k)}}{y_{(n)} - y_{(1)}}, \quad l = 1, \dots, n-1,$$

and with $m_0 = 0$.

With (38) in hand, we let $H_i(t) = D(\widehat{G}_i)(1 - (t - y_{(1)})/(y_{(n)} - y_{(1)}))$ for all $t \in (y_{(1)}, y_{(n)})$. Thus, can write

$$H_i(t) = \sum_{l=1}^{n-1} a_{i,j_l} 1_{[v_l, v_{l-1})}(t)$$

for all $t \in (y_{(1)}, y_{(n)})$, where v_0 and $v_l = y_{(n)} - \sum_{k=1}^l (y_{(j_k+1)} - y_{(j_k)})$ for all $l = 1, \dots, n-1$. Also, $D(\widehat{G}_i)(t) := H((1-t)(y_{(n)} - y_{(1)}) + y_{(1)})$. Hence, from (37) we obtain that

$$\begin{aligned} \frac{1}{y_{(n)} - y_{(1)}} \int_{y_{(1)}}^{y_{(n)}} (H_i(t) - F_i^*(t))^2 dt &= \int_0^1 (D(\widehat{G}_i)(t) - G_i^*(t))^2 dt \\ &\leq \frac{1}{y_{(n)} - y_{(1)}} \int_{y_{(1)}}^{y_{(n)}} (\widehat{F}_i^+(t) - F_i^*(t))^2 dt \end{aligned}$$

and as a result,

$$\int_{y_{(1)}}^{y_{(n)}} (\widetilde{F}_i(t) - F_i^*(t))^2 dt = \int_{y_{(1)}}^{y_{(n)}} (H_i(t) - F_i^*(t))^2 dt \leq \int_{y_{(1)}}^{y_{(n)}} (\widehat{F}_i^+(t) - F_i^*(t))^2 dt, \quad (39)$$

since $H_i(t) = \widetilde{F}_i(t)$ for all $t \in (y_{(1)}, y_{(n)})$.

Combining (29) and (39), we obtain,

$$\int_{\mathbb{R}} (\widetilde{F}_i(t) - F_i^*(t))^2 dt \leq \int_{\mathbb{R}} (\widehat{F}_i^+(t) - F_i^*(t))^2 dt \leq \int_{\mathbb{R}} (\widehat{F}_i(t) - F_i^*(t))^2 dt.$$

The claim then follows.

B.3 Proof of Theorem 2

Proof. First, by the basic inequality we have that

$$\frac{1}{2} \sum_{i=1}^n (F_i(t) - F_i^*(t))^2 \leq \sum_{i=1}^n (F_i^*(t) - 1_{\{y_i \leq t\}})(F_i^*(t) - F_i(t))$$

for all $F \in \{\kappa F^* + (1-\kappa)\widehat{F} : \kappa \in [0, 1]\}$. Hence, for ξ_1, \dots, ξ_n are independent Rademacher random variables, we have that

$$\begin{aligned}
\mathbb{P}\left(\sup_{t \in \mathbb{R}} \sum_{i=1}^n (\widehat{F}_i(t) - F_i^*(t))^2 > 2\eta^2\right) &\leq \mathbb{P}\left(\sup_{t \in \mathbb{R}} \sup_{\theta \in K_t : \|\theta - F^*(t)\| \leq \eta} \sum_{i=1}^n (F_i^*(t) - 1_{\{y_i \leq t\}})(\theta_i - F_i^*(t)) > \eta^2\right) \\
&\leq \mathbb{P}\left(\sup_{t \in \mathbb{R}} \sup_{\theta \in K : \|\theta - F^*(t)\| \leq \eta} \sum_{i=1}^n (F_i^*(t) - 1_{\{y_i \leq t\}})(\theta_i - F_i^*(t)) > \eta^2\right) \\
&\leq \frac{1}{\eta^2} \mathbb{E}\left(\sup_{t \in \mathbb{R}} \sup_{\theta \in K : \|\theta - F^*(t)\| \leq \eta} \sum_{i=1}^n (F_i^*(t) - 1_{\{y_i \leq t\}})(\theta_i - F_i^*(t))\right) \\
&\leq \frac{1}{\eta^2} \mathbb{E}\left(\sup_{t \in \mathbb{R}} \sup_{\theta \in K-K : \|\theta\| \leq \eta} \sum_{i=1}^n (F_i^*(t) - 1_{\{y_i \leq t\}})\theta_i\right) \\
&\leq \frac{2}{\eta^2} \mathbb{E}\left(\sup_{t \in \mathbb{R}} \sup_{\theta \in K-K : \|\theta\| \leq \eta} \sum_{i=1}^n \xi_i 1_{\{y_i \leq t\}} \theta_i\right) \\
&\leq \frac{2}{\eta^2} \mathbb{E}\left(\mathbb{E}\left(\sup_{t \in \mathbb{R}} \sup_{\theta \in K-K : \|\theta\| \leq \eta} \sum_{i=1}^n \xi_i 1_{\{y_i \leq t\}} \theta_i \middle| y\right)\right) \\
&= \frac{2}{\eta^2} \mathbb{E}\left(\mathbb{E}\left(\max_{t \in \{y_1, \dots, y_n\}} \sup_{\theta \in K-K : \|\theta\| \leq \eta} \sum_{i=1}^n \xi_i 1_{\{y_i \leq t\}} \theta_i \middle| y\right)\right)
\end{aligned}$$

where the second inequality follows from Markov's inequality, the fourth by simmetrization. Next, notice that for a fixed t and y , the random variables $\{\xi_i 1_{\{y_i \leq t\}}\}_{i=1}^n$ are subGaussian(1). Hence, by Lemma 3,

$$\mathbb{E}\left(\max_{t \in \{y_1, \dots, y_n\}} \sup_{\theta \in K-K : \|\theta\| \leq \eta} \sum_{i=1}^n \xi_i 1_{\{y_i \leq t\}} \theta_i \middle| y\right) \leq C \int_0^{\eta/4} \sqrt{\log N(\varepsilon, (K-K) \cap B_\varepsilon(0), \|\cdot\|)} d\varepsilon + C\eta\sqrt{\log n},$$

for some constant $C > 0$. The claim then follows. \square

B.4 Proof of Theorem 4

Proof. Following the proof of Theorem 2.2 in Chatterjee (2014), we obtain that for any positive integer l it holds, for $g \sim N(0, I_n)$, that

$$\begin{aligned}
\mathbb{E}\left[\sup_{\theta \in K_t : \|\theta - F^*(t)\| \leq \eta} g^\top (\theta - F^*(t))\right] &= \mathbb{E}\left[\sup_{\theta \in K : \|\theta - F^*(t)\| \leq \eta} g^\top (\theta - F^*(t))\right] \\
&\leq C_1 \left[2\sqrt{2^l \eta n^{1/4}} + \frac{\eta^2}{2^{l-1}}\right]
\end{aligned} \tag{40}$$

for a positive constant C_1 . Next, let L the constant in (4). We now choose l large enough such that

$$\frac{C_1 \eta^2}{2^{l-1}} \leq \frac{\eta^2}{2L}.$$

Furthermore, for this choice of l , we can choose η as $\eta \asymp n^{1/6}$ such that

$$C_1 2\sqrt{2^l \eta} n^{1/4} \leq \frac{\eta^2}{2L}.$$

Thus, for a choice of η satisfying $\eta \asymp n^{1/6}$, we obtain

$$\sup_{t \in \mathbb{R}} \mathbb{E} \left[\sup_{\theta \in K_t : \|\theta - F^*(t)\| \leq \eta} g^\top (\theta - F^*(t)) \right] \leq \frac{\eta^2}{L},$$

and so (9) follows from Theorem 1. Furthermore, the corresponding conclusion for $\{\tilde{F}(t)\}_{t \in \mathbb{R}}$ follows from Corollary 1.

Finally, we notice that for some positive constant C_2

$$\begin{aligned} \int_0^{\eta/4} \sqrt{\log N(\varepsilon, (K \cap [a, b] - K \cap [a, b]) \cap B_\varepsilon(0), \|\cdot\|)} d\varepsilon &\leq 2 \int_0^{\eta/4} \sqrt{\log N(\varepsilon/2, (K \cap [a, b] \cap B_\varepsilon(0), \|\cdot\|))} d\varepsilon \\ &\leq 2 \int_0^{\eta/4} \sqrt{\log N(\varepsilon/2, (K \cap [a, b] \cap B_\varepsilon(0), \|\cdot\|))} d\varepsilon \\ &\leq 2 \int_0^{\eta/4} \sqrt{\frac{2C_2 \sqrt{n}(b-a)}{\varepsilon}} d\varepsilon \\ &\leq 2\sqrt{2C_2(b-a)} n^{1/4} \eta^{1/2} \end{aligned}$$

where the third inequality follows from Lemma 4.20 in Chatterjee (2014). Therefore, the claim in (10) follows from Theorem 2 by taking η satisfying $\eta \asymp (b-a)^{1/3} n^{1/6} + \sqrt{\log n}$. \square

B.5 Proof of Theorem 3

Proof. First we observe that by the basic inequality, for all $t \in \mathbb{R}$,

$$\frac{\|F(t) - F^*(t)\|^2}{2} \leq a(t)^\top (F(t) - F^*(t)) + \lambda_t [\text{pen}_t(F^*(t)) - \text{pen}_t(F(t))] \quad (41)$$

where $a(t) = w(t) - F^*(t)$ for all $t \in \mathbb{R}$ and $i \in \{1, \dots, n\}$, and where the inequality holds for all

$$F(t) \in \Lambda(t) := \left\{ s\widehat{F}(t) + (1-s)F^*(t) : s \in [0, 1] \right\} \subset \mathbb{R}^n.$$

Therefore,

$$\begin{aligned} \text{pen}_t(F(t)) &\leq \text{pen}_t(F(t)) + \frac{\|F(t) - F^*(t)\|^2}{2\lambda_t} \\ &\leq \frac{a(t)^\top (F(t) - F^*(t))}{\lambda_t} + \text{pen}_t(F^*(t)) \end{aligned}$$

for all $F(t) \in \Lambda(t)$ and $t \in \mathbb{R}$. Hence, by the properties of $\text{pen}_t(\cdot)$, we have that

$$\begin{aligned} \text{pen}_t(F(t) - F^*(t)) &\leq \text{pen}_t(F(t)) + \text{pen}_t(F^*(t)) \\ &\leq \frac{a(t)^\top (F(t) - F^*(t))}{\lambda_t} + 2\text{pen}_t(F^*(t)) \end{aligned} \quad (42)$$

for all $F(t) \in \Lambda(t)$ and $t \in \mathbb{R}$.

Now suppose that there exists $F(t) \in \Lambda(t)$ such that

$$\|F(t) - F^*(t)\| \leq \eta^2$$

and $\text{pen}_t(F(t)) \geq 5\text{pen}_t(F^*(t))$. Then

$$\begin{aligned} \text{pen}_t(F(t) - F^*(t)) &\geq \text{pen}_t(F(t)) - \text{pen}_t(F^*(t)) \\ &\geq 4\text{pen}_t(F^*(t)). \end{aligned}$$

Hence, we let

$$s := \frac{4\text{pen}_T(F^*(t))}{\text{pen}_t(F(t) - F^*(t))} \in [0, 1].$$

Then we set

$$\widetilde{F}(t) := sF(t) + (1-s)F^*(t) \in \Lambda(t).$$

As a result,

$$\|F^*(t) - \widetilde{F}(t)\|^2 \leq \|F^*(t) - F(t)\|^2 \leq \eta^2.$$

Also,

$$\begin{aligned} \text{pen}_t(\widetilde{F}(t) - F^*(t)) &= \text{pen}_t(sF(t) + (1-s)F^*(t) - F^*(t)) \\ &= \text{pen}_t(sF(t) - sF^*(t)) \\ &= s\text{pen}_t(F(t) - F^*(t)) \\ &= 4\text{pen}_t(F^*(t)). \end{aligned}$$

Therefore,

$$\begin{aligned} 4\text{pen}_t(F^*(t)) &= \text{pen}_t(\widetilde{F}(t) - F^*(t)) \\ &\leq \frac{a(t)^\top (\widetilde{F}(t) - F^*(t))}{\lambda_t} + 2\text{pen}_t(F^*(t)), \end{aligned}$$

where the inequality follows from (42). This implies that

$$2\text{pen}(F^*(t)) \leq \frac{a(t)^\top (\tilde{F}(t) - F^*(t))}{\lambda_t}. \quad (43)$$

Hence, we let

$$\lambda_t = \frac{\eta^2}{4\text{pen}(F^*(t))}.$$

Then from (43) we obtain that

$$\frac{\eta^2}{2} \leq a(t)^\top (\tilde{F}(t) - F^*(t)).$$

It follows that the events

$$\Omega_1 := \bigcup_{t \in \mathbb{R}} \left\{ \sup_{F(t) \in \Lambda(t) : \|F(t) - F^*(t)\| \leq \eta} \text{pen}_t(F(t)) \geq 5\text{pen}_t(F^*(t)) \right\}$$

and

$$\Omega_2 := \left\{ \sup_{t \in \mathbb{R}} \sup_{F(t) \in \Lambda(t) : \|F(t) - F^*(t)\| \leq \eta, \text{pen}(F^*(t) - F(t)) \leq 4\text{pen}(F^*(t))} a(t)^\top (F(t) - F^*(t)) \geq \frac{\eta^2}{2} \right\}$$

satisfy that $\Omega_1 \subset \Omega_2$. Hence, $\mathbb{P}(\Omega_1) \leq \mathbb{P}(\Omega_2)$.

Next, we observe that if $\|\hat{F}(t) - F(t)\| \geq \eta$, then there exists $F(t) \in \Lambda(t)$ such that $\|F(t) - F^*(t)\| = \eta$. This implies, by (41), that

$$\frac{\eta^2}{2} \leq a(t)^\top (F(t) - F^*(t)) + \lambda_t [\text{pen}(F^*(t)) - \text{pen}(F(t))]$$

and so from our choice of λ_t

$$\frac{\eta^2}{4} \leq a(t)^\top (F(t) - F^*(t)). \quad (44)$$

Thus, (44) holds for some $F(t) \in \Lambda(t)$ with $\|F(t) - F^*(t)\| \leq \eta$ provided that $\|\hat{F}(t) - F^*(t)\| > \eta$. Therefore,

$$\begin{aligned} \mathbb{P} \left(\sup_{t \in \mathbb{R}} \|\hat{F}(t) - F^*(t)\| > \eta \right) &\leq \mathbb{P} \left(\left\{ \sup_{t \in \mathbb{R}} \|\hat{F}(t) - F^*(t)\| > \eta \right\} \cap \Omega_1^c \right) + \mathbb{P}(\Omega_1) \\ &\leq \mathbb{P} \left(\sup_{t \in \mathbb{R}} \sup_{F(t) \in \Lambda(t) : \|F^*(t) - F(t)\| \leq \eta, \text{pen}(F(t)) \leq 5\text{pen}(F^*(t))} a(t)^\top (F(t) - F^*(t)) \right. \\ &\quad \left. \geq \frac{\eta^2}{4} \right) + \mathbb{P}(\Omega_2) \\ &\leq 2 \mathbb{P} \left(\sup_{t \in \mathbb{R}} \sup_{F(t) \in \Lambda(t) : \|F(t) - F^*(t)\| \leq \eta, \text{pen}(F(t)) \leq 5\text{pen}(F^*(t))} a(t)^\top (F(t) - F^*(t)) \right. \\ &\quad \left. \geq \frac{\eta^2}{4} \right) \\ &\leq \frac{8}{\eta^2} \mathbb{E} \left(\sup_{t \in \mathbb{R}} \sup_{F(t) : \|F^*(t) - F(t)\| \leq \eta, \text{pen}(F(t)) \leq 5\text{pen}(F^*(t))} a(t)^\top (F(t) - F^*(t)) \right) \\ &\leq \frac{8}{\eta^2} \mathbb{E} \left(\sup_{t \in \mathbb{R}} \sup_{\theta \in K : \|\theta\| \leq \eta} a(t)^\top \theta \right). \end{aligned} \quad (45)$$

Hence, for ξ_1, \dots, ξ_n independent Rademacher variables independent of y , we have that

$$\begin{aligned}\mathbb{P}\left(\sup_{t \in \mathbb{R}} \|\widehat{F}(t) - F^*(t)\| > \eta\right) &\leq \frac{16}{\eta^2} \mathbb{E}\left(\sup_{t \in \mathbb{R}} \sup_{\theta \in K : \|\theta\| \leq \eta} \sum_{i=1}^n \xi_i 1_{\{y_i \leq t\}} \theta_i\right) \\ &= \frac{16}{\eta^2} \mathbb{E}\left(\mathbb{E}\left(\sup_{t \in \mathbb{R}} \sup_{\theta \in K : \|\theta\| \leq \eta} \sum_{i=1}^n \xi_i 1_{\{y_i \leq t\}} \theta_i \middle| y\right)\right) \\ &= \frac{16}{\eta^2} \mathbb{E}\left(\mathbb{E}\left(\max_{t \in \{y_1, \dots, y_n\}} \sup_{\theta \in K : \|\theta\| \leq \eta} \sum_{i=1}^n \xi_i 1_{\{y_i \leq t\}} \theta_i \middle| y\right)\right)\end{aligned}$$

where the first inequality follows from (45) and symmetrization. However, by Lemma 3,

$$\begin{aligned}\mathbb{E}\left(\max_{t \in \{y_1, \dots, y_n\}} \sup_{\theta \in K : \|\theta\| \leq \eta} \sum_{i=1}^n \xi_i 1_{\{y_i \leq t\}} \theta_i \middle| y\right) &\leq C \int_0^{\eta/4} \sqrt{\log N(\varepsilon, K \cap B_\varepsilon(0), \|\cdot\|)} d\varepsilon \\ &\quad + C\eta\sqrt{\log n},\end{aligned}$$

for some constant $C > 0$. The claim then follows. \square

B.6 Proof of Theorem 5

Let $g \sim N(0, I_n)$ and set

$$K := \left\{ \theta \in \mathbb{R}^n : \text{TV}^{(r)}(\theta) \leq V \right\}. \quad (46)$$

Hence,

$$\begin{aligned}\mathbb{E} \left[\sup_{\theta \in K_t : \|\theta - F^*(t)\| \leq \eta} g^\top (\theta - F^*(t)) \right] &\leq \mathbb{E} \left[\sup_{\theta \in K : \|\theta - F^*(t)\| \leq \eta} g^\top (\theta - F^*(t)) \right] \\ &\leq C_r \left[\eta \left(\frac{\sqrt{n}V}{\eta} \right)^{1/2r} + \eta \sqrt{\log n} \right]\end{aligned} \quad (47)$$

where $C_r > 0$ is a constant the second inequality follows from Lemma B.1 in Guntuboyina et al. (2020).

Next, notice that

$$C_r \eta \left(\frac{\sqrt{n}V}{\eta} \right)^{1/2r} \leq \frac{\eta^2}{2L}$$

holds if

$$(2LC_r)^{2r/(2r+1)} n^{1/(4r+2)} V^{1/(2r+1)} \leq \eta.$$

Also,

$$C_r \eta \sqrt{\log n} \leq \frac{\eta^2}{2L}$$

provided that $2LC_r \sqrt{\log n} \leq \eta$. Hence, taking

$$\eta = \max\{(2LC_r)^{2r/(2r+1)} n^{1/(4r+2)} V^{1/(2r+1)}, 2LC_r \sqrt{\log n}\}$$

we obtain (13).

The claim for $\tilde{F}(t)$ follows from Corollary 1.

To show (14), we observe that by the proof of Theorem B.1 in [Guntuboyina et al. \(2020\)](#), for $0 < \eta < n$, we have

$$\begin{aligned} \int_0^{\eta/4} \sqrt{\log N(\varepsilon, (K - K) \cap B_\varepsilon(0), \|\cdot\|)} d\varepsilon &\leq 2 \int_0^{\eta/4} \sqrt{\log N(\varepsilon/2, K \cap B_\varepsilon(0), \|\cdot\|)} d\varepsilon \\ &\leq \tilde{C}_r \left[\eta \left(\frac{\sqrt{n}V}{\eta} \right)^{1/2r} + \eta \sqrt{\log n} \right] \end{aligned}$$

for some positive constant \tilde{C}_r . Hence, (14) follows with the same argument as above.

B.7 Proof of Theorem 6

Proof. Notice that for any $t \in \mathbb{R}$ we have that

$$\|F(t) - H(t)\|^2 \leq 2nB$$

for all $F(t), H(t) \in K_t$.

Then

$$\begin{aligned} \mathbb{P} \left(\sup_{t \in \mathbb{R}} \|\widehat{F}(t) - G(t)\| > \eta \right) &= \mathbb{P} \left(\sup_{t \in \mathbb{R}} \|\widehat{F}(t) - G(t)\|^2 > \eta^2, \sup_{t \in \mathbb{R}} \|\widehat{F}(t) - G(t)\|^2 \leq 2nB \right) \\ &\leq \sum_{j=1}^J \mathbb{P} \left(\sup_{t \in \mathbb{R}} \|\widehat{F}(t) - G(t)\|^2 > 2^{j-1}\eta^2, \sup_{t \in \mathbb{R}} \|\widehat{F}(t) - G(t)\|^2 \leq 2^j\eta^2 \right) \\ &\leq \sum_{j=1}^J \mathbb{P} \left(\sup_{t \in \mathbb{R}} 2 \sum_{i=1}^n (\widetilde{F}_i(t) - 1_{\{y_i \leq t\}})(G_i(t) - \widehat{F}_i(t)) > 2^{j-1}\eta^2, \right. \\ &\quad \left. \sup_{t \in \mathbb{R}} \|\widehat{F}(t) - G(t)\|^2 \leq 2^j\eta^2 \right) \\ &\leq \sum_{j=1}^J \mathbb{P} \left(\sup_{t \in \mathbb{R}} \sup_{F(t) \in K_t : \|F(t) - G(t)\|^2 \leq 2^j\eta^2} \sum_{i=1}^n (G_i(t) - 1_{\{y_i \leq t\}})(G_i(t) - F_i(t)) \right. \\ &\quad \left. > 2^{j-2}\eta^2 \right) \end{aligned}$$

where the first inequality follows by union bound, the second by the basic inequality. However,

$$\begin{aligned} &\mathbb{P} \left(\sup_{t \in \mathbb{R}} \sup_{F(t) \in K_t : \|F(t) - G(t)\|^2 \leq 2^j\eta^2} \sum_{i=1}^n (G_i(t) - 1_{\{y_i \leq t\}})(G_i(t) - F_i(t)) > 2^{j-2}\eta^2 \right) \\ &\leq \frac{1}{2^{j-2}\eta^2} \mathbb{E} \left(\sup_{t \in \mathbb{R}} \sup_{F(t) \in K_t : \|F(t) - G(t)\|^2 \leq 2^j\eta^2} \sum_{i=1}^n (G_i(t) - 1_{\{y_i \leq t\}})(G_i(t) - F_i(t)) \right) \\ &\leq \frac{1}{2^{j-2}\eta^2} \mathbb{E} \left(\sup_{t \in \mathbb{R}} \sup_{F(t) \in K_t : \|F(t) - G(t)\|^2 \leq 2^j\eta^2} \sum_{i=1}^n (F_i^*(t) - 1_{\{y_i \leq t\}})(G_i(t) - F_i(t)) \right) \\ &\quad + \frac{1}{2^{j-2}\eta^2} \sup_{t \in \mathbb{R}} \sup_{F(t) \in K_t : \|F(t) - G(t)\|^2 \leq 2^j\eta^2} \sum_{i=1}^n (G_i(t) - F_i^*(t))(G_i(t) - F_i(t)) \\ &\leq \frac{1}{2^{j-2}\eta^2} \mathbb{E} \left(\sup_{t \in \mathbb{R}} \sup_{F(t) \in K_t : \|F(t) - G(t)\|^2 \leq 2^j\eta^2} \sum_{i=1}^n (F_i^*(t) - 1_{\{y_i \leq t\}})(G_i(t) - F_i(t)) \right) \\ &\quad + \frac{4\sqrt{n}}{2^{j/2}\eta} \sup_{t \in \mathbb{R}} \|G(t) - F^*(t)\|_\infty \end{aligned}$$

for some constant $C > 0$, where the first inequality follows from Markov's inequality, and the last inequality holds by Cauchy–Schwarz inequality. Furthermore,

$$\begin{aligned} & \mathbb{E} \left(\sup_{t \in \mathbb{R}} \sup_{F(t) \in K_t : \|F(t) - G(t)\|^2 \leq 2^j \eta^2} \sum_{i=1}^n (F_i^*(t) - 1_{\{y_i \leq t\}})(G_i(t) - F_i(t)) \right) \\ & \leq \mathbb{E} \left(\sup_{t \in \mathbb{R}} \sup_{F(t) \in K_t - K_t : \|F(t)\|^2 \leq 2^j \eta^2} \sum_{i=1}^n (F_i^*(t) - 1_{\{y_i \leq t\}})F_i(t) \right) \\ & \leq C \int_0^{2^{j/2}\eta/4} \sqrt{\log N(\varepsilon, (K - K) \cap B_\varepsilon(0), \|\cdot\|)} d\varepsilon + C 2^{j/2} \eta \sqrt{\log n}, \end{aligned}$$

where the last inequality follows as in the proof of Theorem 2. Therefore,

$$\begin{aligned} \mathbb{P} \left(\sup_{t \in \mathbb{R}} \|\widehat{F}(t) - G(t)\| > \eta \right) & \leq \sum_{j=1}^J \frac{1}{2^{j-2}\eta^2} \left[C \int_0^{2^{j/2}\eta/4} \sqrt{\log N(\varepsilon, (K - K) \cap B_\varepsilon(0), \|\cdot\|)} d\varepsilon \right. \\ & \quad \left. + C 2^{j/2} \eta \sqrt{\log n} \right] + \sum_{j=1}^J \frac{4\sqrt{n}}{2^{j/2}\eta} \sup_{t \in \mathbb{R}} \|G(t) - F^*(t)\|_\infty \\ & \leq \frac{C}{\eta^2} \sum_{j=1}^J \frac{1}{2^{j-2}} \int_0^{2^{j/2}\eta/4} \sqrt{\log N(\varepsilon, (K - K) \cap B_\varepsilon(0), \|\cdot\|)} d\varepsilon + \\ & \quad \frac{4C\sqrt{\log n}}{\eta} \sum_{j=1}^J \left(\frac{1}{2^{1/2}} \right)^j + \frac{4\sqrt{n}}{\eta} \sup_{t \in \mathbb{R}} \|G(t) - F^*(t)\|_\infty \sum_{j=1}^J \left(\frac{1}{2^{1/2}} \right)^j \\ & \leq \frac{C}{\eta^2} \sum_{j=1}^J \frac{1}{2^{j-2}} \int_0^{2^{j/2}\eta/4} \sqrt{\log N(\varepsilon, (K - K) \cap B_\varepsilon(0), \|\cdot\|)} d\varepsilon + \\ & \quad \frac{4C\sqrt{\log n}}{\eta} \frac{2^{-1/2}}{1 - 2^{-1/2}} + \frac{4\sqrt{n}}{\eta} \sup_{t \in \mathbb{R}} \|G(t) - F^*(t)\|_\infty \frac{2^{-1/2}}{1 - 2^{-1/2}} \end{aligned}$$

and the claim follows noticing that

$$\mathbb{P} \left(\sup_{t \in \mathbb{R}} \|\widehat{F}(t) - F^*(t)\| > \eta + \sqrt{n} \|F^*(t) - G(t)\|_\infty \right) \leq \mathbb{P} \left(\sup_{t \in \mathbb{R}} \|\widehat{F}(t) - G(t)\| > \eta \right).$$

□

B.8 Proof of Theorem 7

We proceed by using Theorem 6. First, for a vector $v \in \mathbb{R}^n$, we let $\|v\|_n := \|v\|/\sqrt{n}$. Then, by Theorem 3 in Kohler and Langer (2021), it holds that

$$\sup_{t \in \mathbb{R}} \|F^*(t) - G(t)\|_\infty \leq C_1 \sqrt{\phi_n}. \quad (48)$$

for some positive constant C_1 .

Furthermore, as in the proof of Theorem 2 in Zhang et al. (2024), see also Lemma 19 in Kohler and Langer (2021), we have that

$$\log N(\varepsilon, \mathcal{F}(L, \nu), \|\cdot\|_n) \lesssim L^2 \nu^2 \log(L\nu) \log(\varepsilon^{-1})$$

for $\varepsilon \in (0, 1)$. Therefore, for $\epsilon \in (0, 2\sqrt{n})$, we have that

$$\log N(\varepsilon, \mathcal{F}(L, \nu), \|\cdot\|) \lesssim L^2 \nu^2 \log(L\nu) \log(2\varepsilon^{-1}\sqrt{n}).$$

Therefore, for $\eta < \sqrt{n}$, with

$$J = \left\lceil \frac{\log(2n/\eta^2)}{\log 2} \right\rceil,$$

it holds that

$$\begin{aligned} & \frac{C}{\eta^2} \sum_{j=1}^J \frac{1}{2^{j-2}} \int_0^{2^{j/2}\eta/4} \sqrt{\log N(\varepsilon, K(\varepsilon), \|\cdot\|)} d\varepsilon + \frac{C\sqrt{\log n}}{\eta} + \frac{C\sqrt{n}}{\eta} \sup_{t \in \mathbb{R}} \|G(t) - F^*(t)\|_\infty \\ & \leq \frac{C}{\eta^2} \sum_{j=1}^J \frac{1}{2^{j-2}} \int_0^{2^{j/2}\eta/4} \sqrt{\log N(\varepsilon, K - K, \|\cdot\|)} d\varepsilon + \frac{C\sqrt{\log n}}{\eta} + \frac{C\sqrt{n}}{\eta} \sup_{t \in \mathbb{R}} \|G(t) - F^*(t)\|_\infty \\ & \leq \frac{C}{\eta^2} \sum_{j=1}^J \frac{1}{2^{j-2}} \int_0^{2^{j/2}\eta/4} \sqrt{\log N(\varepsilon, K - K, \|\cdot\|)} d\varepsilon + \frac{CC_1\sqrt{\log n}}{\eta} + \frac{C\sqrt{n\phi_n}}{\eta} \\ & \lesssim \frac{1}{\eta^2} \sum_{j=1}^J \frac{1}{2^{j-2}} \int_0^{2^{j/2}\eta/4} \sqrt{\log N(\varepsilon/2, K, \|\cdot\|)} d\varepsilon + \frac{\sqrt{\log n}}{\eta} + \frac{\sqrt{n\phi_n}}{\eta} \\ & \lesssim \frac{1}{\eta^2} \sum_{j=1}^J \frac{1}{2^{j-2}} \int_0^{2^{j/2}\eta/4} \sqrt{L^2 \nu^2 \log(L\nu) \log(4\varepsilon^{-1}\sqrt{n})} d\varepsilon + \frac{\sqrt{\log n}}{\eta} + \frac{\sqrt{n\phi_n}}{\eta} \\ & \leq \frac{L\nu\sqrt{\log(L\nu)}}{\eta^2} \sum_{j=1}^J \frac{1}{2^{j-2}} \int_0^{2^{j/2}\eta/4} \sqrt{\log(n) + 4\varepsilon^{-1}} d\varepsilon + \frac{\sqrt{\log n}}{\eta} + \frac{\sqrt{n\phi_n}}{\eta} \\ & \leq \frac{L\nu\sqrt{\log(L\nu)}}{\eta^2} \sum_{j=1}^J \frac{1}{2^{j-2}} \int_0^{2^{j/2}\eta/4} (\sqrt{\log(n)} + 2\varepsilon^{-1/2}) d\varepsilon + \frac{\sqrt{\log n}}{\eta} + \frac{\sqrt{n\phi_n}}{\eta} \\ & \leq \frac{L\nu\sqrt{\log(L\nu)}}{\eta^2} \sum_{j=1}^J \frac{4\eta\sqrt{\log n}}{2^{j/2}} + \frac{L\nu\sqrt{\log(L\nu)}}{\eta^2} \sum_{j=1}^J \frac{1}{2^{j-2}} \int_0^{2^{j/2}\eta/4} 2\varepsilon^{-1/2} d\varepsilon + \frac{\sqrt{\log n}}{\eta} + \frac{\sqrt{n\phi_n}}{\eta} \\ & \lesssim \frac{L\nu\sqrt{\log(L\nu)\log n}}{\eta} + \frac{L\nu\sqrt{\log(L\nu)}}{\eta^2} \sum_{j=1}^J \frac{1}{2^{j-2}} \int_0^{2^{j/2}\eta/4} 2\varepsilon^{-1/2} d\varepsilon + \frac{\sqrt{\log n}}{\eta} + \frac{\sqrt{n\phi_n}}{\eta} \\ & \lesssim \frac{L\nu\sqrt{\log(L\nu)\log n}}{\eta} + \frac{L\nu\sqrt{\log(L\nu)}}{\eta^2} \sum_{j=1}^J \frac{\sqrt{\eta}}{2^{3j/4-2}} + \frac{\sqrt{\log n}}{\eta} + \frac{\sqrt{n\phi_n}}{\eta}. \\ & \lesssim \frac{L\nu\sqrt{\log(L\nu)\log n}}{\eta} + \frac{L\nu\sqrt{\log(L\nu)}}{\eta^{3/2}} + \frac{\sqrt{\log n}}{\eta} + \frac{\sqrt{n\phi_n}}{\eta}. \end{aligned} \tag{49}$$

Moreover, by our choice of L and ν ,

$$L\nu \asymp (\log n) \cdot \sqrt{n\phi_n}. \tag{50}$$

Therefore, from (49) and (50),

$$\begin{aligned} & \frac{C}{\eta^2} \sum_{j=1}^J \frac{1}{2^{j-2}} \int_0^{2^{j/2}\eta/4} \sqrt{\log N(\varepsilon, K(\varepsilon), \|\cdot\|)} d\varepsilon + \frac{C\sqrt{\log n}}{\eta} + \frac{C\sqrt{n}}{\eta} \sup_{t \in \mathbb{R}} \|G(t) - F^*(t)\|_\infty \\ & \lesssim \frac{\sqrt{n\phi_n} \log^2 n}{\eta} + \frac{\sqrt{n\phi_n \log(n)}}{\eta^{3/2}} + \frac{\sqrt{\log n}}{\eta} + \frac{\sqrt{n\phi_n}}{\eta}. \end{aligned} \tag{51}$$

Hence, the claim follows by taking

$$\eta \asymp \sqrt{\log n} + \sqrt{n\phi_n} \log^2 n.$$

B.9 Auxiliary Lemmas

Definition 3. Let $K \subset \mathbb{R}^n$ and $t > 0$. A subset P of K is a packing of K if $P \subset K$ and the set $\{B_t(x)\}_{x \in P}$ is pairwise disjoint. Then, the t -packing number of K , denoted as $M(t, K, \|\cdot\|)$, is defined as the cardinality of any maximum t -packing.

Lemma 2. [Variant of Dudley's inequality.] Let $S \subset \mathbb{R}^n$ be a finite set and $\epsilon^{(j)} \in \mathbb{R}^n$ be a vector of mean zero independent SubGaussian(1) random variables, for $j = 1 \dots, m$. Suppose that $0 \in S$ and $v \in S$ implies that $\|v\| \leq D_n/2$ for some $D_n > 0$. Then there exists a constant $C > 0$ such that

$$\mathbb{E} \left(\max_{j=1,\dots,m} \max_{v \in S} v^\top \epsilon^{(j)} \right) \leq C \left(D_n \sqrt{\log m} + \int_0^{D_n/4} \sqrt{\log M(\delta, S, \|\cdot\|)} d\delta \right)$$

where $M(\delta, S, \|\cdot\|)$ is the packing number of S with respect to the metric $\|\cdot\|$.

Proof. For $C \geq 1$, let S_n be a maximal $D_n 2^{-l}$ -separated subset of S , i.e.,

$$\min_{v,u \in S} \|v - u\| > D_n 2^{-l}.$$

By construction, $|S_l| = M(D_n 2^{-l}, S, \|\cdot\|)$. Clearly, because of the maximality,

$$\max_{v \in S} \min_{u \in S_l} \|v - u\| \leq D_n 2^{-l}.$$

Furthermore, $S_l = S$ for large enough l . Hence, we let

$$N = \min \{l \geq 1 : S_l = S\}.$$

Also, for $l \geq 1$, let π_l be the function that assigns $v \in S$ to the point in S_l closest to v . By definition,

$$\|\pi_l(v) - v\| \leq D 2^{-l}$$

for all $v \in S$ and $l \in \mathbb{N}$. We also write $S_0 = \{0\}$ and so $\pi_0(v) = 0$ for all $v \in S$. Next, we observe that

$$v^\top \epsilon^{(j)} = \sum_{l=1}^N (\pi_l(v) - \pi_{l-1}(v))^\top \epsilon^{(j)}$$

for all $v \in S$. It follows that

$$\begin{aligned} \max_{j=1,\dots,m} \max_{v \in S} v^\top \epsilon^{(j)} &\leq \max_{j=1,\dots,m} \max_{v \in S} \sum_{l=1}^N (\pi_l(v) - \pi_{l-1}(v))^\top \epsilon^{(j)} \\ &\leq \sum_{l=1}^N \max_{j=1,\dots,m} \max_{v \in S} (\pi_l(v) - \pi_{l-1}(v))^\top \epsilon^{(j)} \end{aligned}$$

and so

$$\mathbb{E} \left(\max_{j=1,\dots,m} \max_{v \in S} v^\top \epsilon^{(j)} \right) \leq \sum_{l=1}^N \mathbb{E} \left(\max_{j=1,\dots,m} \max_{v \in S} (\pi_l(v) - \pi_{l-1}(v))^\top \epsilon^{(j)} \right).$$

However, notice that for all $u > 0$,

$$\mathbb{P} \left((\pi_l(v) - \pi_{l-1}(v))^\top \epsilon^{(j)} \geq u \right) \leq 2 \exp \left(\frac{-u^2}{2\|\pi_l(v) - \pi_{l-1}(v)\|^2} \right)$$

and

$$\begin{aligned} \|\pi_l(v) - \pi_{l-1}(v)\| &\leq \|\pi_l(v) - v\| + \|\pi_{l-1}(v) - v\| \\ &\leq D_n 2^{-l} + D_n 2^{l-1} \\ &\leq 3D_n 2^{-l} \end{aligned}$$

which implies, by the subGaussian maximal inequality, that

$$\begin{aligned} \mathbb{E} \left(\max_{j=1,\dots,m} \max_{v \in S} (\pi_l(v) - \pi_{l-1}(v))^\top \epsilon^{(j)} \right) &\leq \frac{3CD_n}{2^l} \sqrt{\log(2m|S_l||S_{l-1}|)} \\ &\leq \frac{3CD_n}{2^l} \sqrt{\log(2m|S_l|^2)} \\ &\leq \frac{3CD_n}{2^l} \sqrt{\log(2mM(D2^{-l}, S, \|\cdot\|))} \end{aligned}$$

for some constant $C > 0$. Therefore,

$$\begin{aligned} \mathbb{E} \left(\max_{j=1,\dots,m} \max_{v \in S} v^\top \epsilon^{(j)} \right) &\leq 3C \sum_{l=1}^N \frac{D_n}{2^l} \sqrt{\log m + \log(2M(D_n 2^l, S, \|\cdot\|))} \\ &\leq 3C \sqrt{\log m} \sum_{l=1}^N \frac{D_n}{2^l} + 3C \sum_{l=1}^N \frac{D_n}{2^l} \sqrt{\log(2M(D 2^{-l}, S, \|\cdot\|))} \\ &\leq 3CD_n \sqrt{\log m} + 3C \sum_{l=1}^N \frac{D_n}{2^l} \sqrt{\log(2M(D_n 2^{-l}, S, \|\cdot\|))} \\ &\leq 3CD_n \sqrt{\log m} + 6C \sum_{l=1}^N \int_{D_n/2^{l+1}}^{D/2^l} \sqrt{\log(2M(r, S, \|\cdot\|))} dr \\ &= 3CD_n \sqrt{\log m} + 6C \int_{D_n/2^{N+1}}^{D/2} \sqrt{\log(2M(r, S, \|\cdot\|))} dr \\ &\leq 3CD_n \sqrt{\log m} + 6C \int_0^{D_n/2} \sqrt{\log(2M(r, S, \|\cdot\|))} dr \\ &\leq 3CD_n \sqrt{\log m} + 6C \int_0^{D_n/4} \sqrt{\log(2M(r, S, \|\cdot\|))} dr \\ &\quad + 6C \int_0^{D_n/4} \sqrt{\log(2M(r + D_n/4, S, \|\cdot\|))} dr \\ &\leq 3CD_n \sqrt{\log m} + 12C \int_0^{D_n/4} \sqrt{\log(2M(r, S, \|\cdot\|))} dr \\ &\leq 3CD_n \sqrt{\log m} + 24C \int_0^{D_n/4} \sqrt{\log(M(r, S, \|\cdot\|))} dr \end{aligned}$$

and the claim follows. \square

Lemma 3. *With the notation and conditions of Lemma 2, if $S \subset \mathbb{R}$ arbitrary (not necessarily finite), then*

$$\mathbb{E} \left(\max_{j=1,\dots,m} \sup_{v \in S} v^\top \epsilon^{(j)} \right) \leq C \left(D_n \sqrt{\log m} + \int_0^{D_n/4} \sqrt{\log M(\delta, S, \|\cdot\|)} d\delta \right).$$

Proof. Let $\tilde{S} \subset S$ be a countable set such that

$$\max_{j=1,\dots,m} \sup_{v \in S} v^\top \epsilon^{(j)} = \max_{j=1,\dots,m} \sup_{v \in \tilde{S}} v^\top \epsilon^{(j)}.$$

Let \tilde{S}_l the set consisting of the first l elements of \tilde{S} . Without loss of generality let's assume that $0 \in \tilde{S}_l$ for all l . Then by Lemma 2, we have that

$$\begin{aligned} \mathbb{E} \left(\max_{j=1,\dots,m} \sup_{v \in \tilde{S}_l} v^\top \epsilon^{(j)} \right) &\leq C \left(D_n \sqrt{\log m} + \int_0^{D_n/4} \sqrt{\log M(\delta, \tilde{S}_l, \|\cdot\|)} d\delta \right) \\ &\leq C \left(D_n \sqrt{\log m} + \int_0^{D_n/4} \sqrt{\log M(\delta, S, \|\cdot\|)} d\delta \right) \end{aligned} \quad (52)$$

for all $l \geq 1$. Hence, the claim follows by letting $l \rightarrow \infty$ in (52) and applying the Monotone Convergence Theorem. \square

Definition 4. *For $t \in \mathbb{R}$ let $\epsilon(t) = w(t) - F^*(t) \in \mathbb{R}^n$. Then for a set $\mathcal{V} \subset \mathbb{R}^n$ define*

$$R_t(\mathcal{V}) = \mathbb{E} \left(\sup_{v \in \mathcal{V}} \sum_{i=1}^n v_i \epsilon_i(t) \right).$$

Furthermore, define the Gaussian complexity of \mathcal{V} as

$$\mathcal{R}(\mathcal{V}) = \mathbb{E} \left(\sup_{v \in \mathcal{V}} \sum_{i=1}^n v_i g_i \right),$$

where $g \sim N(0, I)$.

Lemma 4. *There exists a universal constant such that for any set $\mathcal{V} \subset \mathbb{R}^n$ it holds that*

$$\sup_{t \in \mathbb{R}} R_t(\mathcal{V}) \leq L \mathcal{R}(\mathcal{V}),$$

where $L > 0$ is a universal constant.

Proof. Fix $t \in \mathbb{R}$. Then for $v \in \mathcal{V}$, let $Y_v = v^\top \epsilon(t)$ and $X_v = v^\top g$. Next, observe that

$$\sup_{u,v \in \mathcal{V}} |Y_u - Y_v| = \sup_{u,v \in \mathcal{V}} (Y_u - Y_v) = \sup_{u \in \mathcal{V}} Y_u + \sup_{v \in \mathcal{V}} -Y_v.$$

Hence, for any $v_0 \in \mathcal{V}$,

$$\begin{aligned} \mathbb{E} \left(\sup_{u,v \in \mathcal{V}} |Y_u - Y_v| \right) &= \mathbb{E} \left(\sup_{u \in \mathcal{V}} Y_u \right) + \mathbb{E} \left(\sup_{v \in \mathcal{V}} -Y_v \right) \\ &\geq \mathbb{E} \left(\sup_{u \in \mathcal{V}} Y_u \right) + \mathbb{E} (-Y_{v_0}) \\ &\geq \mathbb{E} \left(\sup_{u \in \mathcal{V}} Y_u \right) \\ &= R_t(\mathcal{V}). \end{aligned} \quad (53)$$

Now, we observe that $\epsilon_i(t)$ is sub-Gaussian(1). Hence, by Theorem 2.1.5 from [Talagrand \(2005\)](#), we have that

$$\mathbb{E} \left(\sup_{u,v \in \mathcal{V}} |Y_u - Y_v| \right) \leq L \mathbb{E}(\sup_{v \in \mathcal{V}} v^\top g) = L \mathcal{R}(\mathcal{V}),$$

for a universal constant that does not depend on t . Hence, the claim follows. \square

Definition 5. For a measurable function $f : \mathbb{R} \rightarrow \mathbb{R}$ we define its distribution with respect to the Lebesgue measure as the function $\mu_f : [0, \infty) \rightarrow \mathbb{R}$ given as

$$\mu_f(\lambda) := \mu(\{x : |f(x)| > \lambda\})$$

where μ is the Lebesgue measure.

Definition 6. For a measurable function $f : \mathbb{R} \rightarrow \mathbb{R}$ we define its decreasing rearrangement $D(f) : [0, \infty) \rightarrow \mathbb{R}$ given as

$$D(f)(t) := \inf\{\lambda \geq 0 : \mu_f(\lambda) \leq t\}$$

where μ is the Lebesgue measure.

Lemma 5. Suppose that f can be written as

$$f(t) = \sum_{l=1}^{n-1} b_l 1_{E_l}(t)$$

for $b_1 \geq \dots \geq b_{n-1} \geq 0$ and measurable sets $E_l \subset \mathbb{R}$ that are pairwise disjoint. Then the decreasing rearrangement of f is given by

$$D(f)(t) = \sum_{l=1}^{n-1} b_l 1_{[m_{l-1}, m_l)}(t)$$

where

$$m_l := \sum_{k=1}^l \mu(E_k), \quad l = 1, \dots, n-1,$$

and with $m_0 = 0$.

Proof. This is Example 1.6 in [Bennett and Sharpley \(1988\)](#). \square

Lemma 6. For any integrable functions f and g the following hold:

1.

$$\int_{\mathbb{R}} |f(t)|^2 dt = \int_0^\infty |D(f)(t)|^2 dt. \tag{54}$$

2. [G.H. Hardy and J.E. Littlewood].

$$\int_{\mathbb{R}} |f(t)g(t)| dt \leq \int_0^\infty D(f)(s) \cdot D(g)(s) ds. \tag{55}$$

3. Suppose that f is decreasing and continuous in $[0, a)$ for some $a > 0$, and $f(t) = 0$ otherwise. Then $f(t) = D(f)(t)$ for all $t \in [0, \infty)$.

Proof. The claim in (54) follows from Proposition 1.8 in Bennett and Sharpley (1988). The inequality in (55) is the well-known G.H Hardy and J.E Littlewood inequality, see for instance Theorem 2.2 in Bennett and Sharpley (1988).

We now prove the final claim. Let $t \geq 0$. Suppose that $t \in [0, a)$. Then

$$\begin{aligned} D(f)(t) &= \inf\{\lambda \geq 0 : \sup\{x : f(x) > \lambda\} \leq t\} \\ &= \inf\{\lambda \geq 0 : \sup\{x \geq 0 : f(x) > \lambda\} \leq t\}. \end{aligned} \quad (56)$$

Hence, for $0 \leq \lambda < f(t)$, the continuity of f in $[0, a)$, implies that there exists $t' \in (t, a)$ such that $\lambda < f(t') \leq f(t)$. Thus, $\sup\{x \geq 0 : f(x) > \lambda\} > t$. On the other hand, if $f(0) \geq \lambda \geq f(t)$, then, also by the continuity of f in $[0, a)$,

$$\sup\{x \geq 0 : f(x) > \lambda\} = \inf\{x \geq 0 : f(x) = \lambda\}.$$

Hence, from (56), we obtain $f(t) = D(f)(t)$ for $t \in [0, a)$.

Suppose now that $t \in [a, \infty)$. Then

$$\mu_f(0) \leq a \leq t.$$

Hence, $D(f)(t) = 0$ and the claim follows. \square

References

- Richard E Barlow and Hugh D Brunk. The isotonic regression problem and its dual. *Journal of the American Statistical Association*, 67(337):140–147, 1972.
- Richard E Barlow, David J Bartholomew, John M Bremner, and H Dale Brunk. *Statistical inference under order restrictions: The theory and application of isotonic regression*. Wiley, 1972.
- Benedikt Bauer and Michael Kohler. On deep learning as a remedy for the curse of dimensionality in nonparametric regression. 2019.
- Colin Bennett and Robert C Sharpley. *Interpolation of operators*. Academic press, 1988.
- Leo Breiman. Random forests. *Machine learning*, 45:5–32, 2001.
- Leo Breiman, Jerome Friedman, and Charles J Stone. e richard a olshen, 1984.
- Hugh D Brunk. *Estimation of isotonic regression*. University of Missouri-Columbia, 1969.
- Domagoj Cevid, Loris Michel, Jeffrey Naf, Peter Bühlmann, and Nicolai Meinshausen. Distributional random forests: Heterogeneity adjustment and multivariate distributional regression. *Journal of Machine Learning Research*, 23(333):1–79, 2022.
- Sabyasachi Chatterjee and Subhajit Goswami. New risk bounds for 2d total variation denoising. *IEEE Transactions on Information Theory*, 67(6):4060–4091, 2021.
- Sabyasachi Chatterjee, Adityanand Guntuboyina, and Bodhisattva Sen. On risk bounds in isotonic and other shape restricted regression problems. 2015.
- Sourav Chatterjee. A new perspective on least squares under convex constraint. 2014.
- Victor Chernozhukov, Iván Fernández-Val, and Blaise Melly. Inference on counterfactual distributions. *Econometrica*, 81(6):2205–2268, 2013.
- Ori Davidov and George Iliopoulos. Estimating a distribution function subject to a stochastic order restriction: a comparative study. *Journal of Nonparametric Statistics*, 24(4):923–933, 2012.
- David B Dunson, Natesh Pillai, and Ju-Hyun Park. Bayesian density regression. *Journal of the Royal Statistical Society Series B: Statistical Methodology*, 69(2):163–183, 2007.
- Hammou El Barmi and Hari Mukerjee. Inferences under a stochastic ordering constraint: the k-sample case. *Journal of the American Statistical Association*, 100(469):252–261, 2005.
- Sergio Firpo and Stefanie Sunao. Decomposition methods. In *Handbook of Labor, Human Resources and Population Economics*, pages 1–32. Springer, 2023.
- Silverio Foresi and Franco Peracchi. The conditional distribution of excess returns: An empirical analysis. *Journal of the American Statistical Association*, 90(430):451–466, 1995.
- Jerome H Friedman. Multivariate adaptive regression splines. *The annals of statistics*, 19(1):1–67, 1991.

- Tilmann Gneiting and Adrian E. Raftery. Strictly proper scoring rules, prediction, and estimation. *Journal of the American Statistical Association*, 102(477):359–378, 2007.
- Adityanand Guntuboyina, Donovan Lieu, Sabyasachi Chatterjee, and Bodhisattva Sen. Adaptive risk bounds in univariate total variation denoising and trend filtering. *The Annals of Statistics*, 48:205–229, 2020.
- Peter Hall, Rodney CL Wolff, and Qiwei Yao. Methods for estimating a conditional distribution function. *Journal of the American Statistical association*, 94(445):154–163, 1999.
- Trevor Hastie, Robert Tibshirani, and Jerome Friedman. *The Elements of Statistical Learning: Data Mining, Inference, and Prediction*. Springer, New York, 2nd edition, 2009. ISBN 978-0387848570.
- Alexander Henzi, Johanna F Ziegel, and Tilmann Gneiting. Isotonic distributional regression. *Journal of the Royal Statistical Society Series B: Statistical Methodology*, 83(5):963–993, 2021.
- Robert V Hogg. On models and hypotheses with restricted alternatives. *Journal of the American Statistical Association*, 60(312):1153–1162, 1965.
- Jan-Christian Hütter and Philippe Rigollet. Optimal rates for total variation denoising. In *Conference on Learning Theory*, pages 1115–1146. PMLR, 2016.
- Ehsan Imani and Martha White. Improving regression performance with distributional losses. In *International conference on machine learning*, pages 2157–2166. PMLR, 2018.
- Javier Rojo Jiménez and Hammou El Barmi. Estimation of distribution functions under second order stochastic dominance. *Statistica Sinica*, pages 903–926, 2003.
- Nadja Klein. Distributional regression for data analysis. *Annual Review of Statistics and Its Application*, 11, 2024.
- Thomas Kneib, Alexander Silbersdorff, and Benjamin Säfken. Rage against the mean—a review of distributional regression approaches. *Econometrics and Statistics*, 26:99–123, 2023.
- Roger Koenker and Gilbert Bassett Jr. Regression quantiles. *Econometrica: journal of the Econometric Society*, pages 33–50, 1978.
- Roger Koenker, Samantha Leorato, and Franco Peracchi. Distributional vs. quantile regression. 2013.
- Michael Kohler and Sophie Langer. On the rate of convergence of fully connected deep neural network regression estimates. *The Annals of Statistics*, 49(4):2231–2249, 2021.
- Kevin Lin, James L Sharpnack, Alessandro Rinaldo, and Ryan J Tibshirani. A sharp error analysis for the fused lasso, with application to approximate changepoint screening. *Advances in neural information processing systems*, 30, 2017.
- Georg Gunther Lorentz. An inequality for rearrangements. *The American Mathematical Monthly*, 60(3):176–179, 1953.

- Mingliang Ma and Abolfazl Safikhani. Theoretical analysis of deep neural networks for temporally dependent observations. *Advances in Neural Information Processing Systems*, 35:37324–37334, 2022.
- Oscar Hernan Madrid Padilla and Sabyasachi Chatterjee. Risk bounds for quantile trend filtering. *Biometrika*, 109(3):751–768, 2022.
- Enno Mammen and Sara Van De Geer. Locally adaptive regression splines. *The Annals of Statistics*, 25(1):387–413, 1997.
- Alexandre Mösching and Lutz Dümbgen. Monotone least squares and isotonic quantiles. 2020.
- R Kelley Pace and Ronald Barry. Sparse spatial autoregressions. *Statistics & Probability Letters*, 33(3):291–297, 1997.
- Carlos Misael Madrid Padilla, Oscar Hernan Madrid Padilla, and Daren Wang. Temporal-spatial model via trend filtering. *arXiv preprint arXiv:2308.16172*, 2023.
- Carlos Misael Madrid Padilla, Oscar Hernan Madrid Padilla, Yik Lun Kei, Zhi Zhang, and Yanzhen Chen. Confidence interval construction and conditional variance estimation with dense relu networks. *arXiv preprint arXiv:2412.20355*, 2024.
- Oscar Hernan Madrid Padilla, James Sharpnack, James G Scott, and Ryan J Tibshirani. The dfs fused lasso: Linear-time denoising over general graphs. *Journal of Machine Learning Research*, 18(176):1–36, 2018.
- Oscar Hernan Madrid Padilla, Wesley Tansey, and Yanzhen Chen. Quantile regression with relu networks: Estimators and minimax rates. *Journal of Machine Learning Research*, 23(247):1–42, 2022.
- Franco Peracchi. On estimating conditional quantiles and distribution functions. *Computational statistics & data analysis*, 38(4):433–447, 2002.
- Tim Robertson. Order restricted statistical inference/[et al.]. 1988.
- Christoph Rothe. Partial distributional policy effects. *Econometrica*, 80(5):2269–2301, 2012.
- Christoph Rothe and Dominik Wied. Misspecification testing in a class of conditional distributional models. *Journal of the American Statistical Association*, 108(501):314–324, 2013.
- Leonid I Rudin, Stanley Osher, and Emad Fatemi. Nonlinear total variation based noise removal algorithms. *Physica D: nonlinear phenomena*, 60(1-4):259–268, 1992.
- Lisa Schlosser, Torsten Hothorn, Reto Stauffer, and Achim Zeileis. Distributional regression forests for probabilistic precipitation forecasting in complex terrain. 2019.
- Johannes Schmidt-Hieber. Nonparametric regression using deep neural networks with relu activation function. 2020.
- Xinwei Shen and Nicolai Meinshausen. Engrssion: extrapolation through the lens of distributional regression. *Journal of the Royal Statistical Society Series B: Statistical Methodology*, page qkae108, 2024.

Michel Talagrand. *The generic chaining: upper and lower bounds of stochastic processes*. Springer Science & Business Media, 2005.

Wesley Tansey, Jesse Thomason, and James Scott. Maximum-variance total variation denoising for interpretable spatial smoothing. In *Proceedings of the AAAI Conference on Artificial Intelligence*, volume 32, 2018.

Robert Tibshirani, Michael Saunders, Saharon Rosset, Ji Zhu, and Keith Knight. Sparsity and smoothness via the fused lasso. *Journal of the Royal Statistical Society: Series B (Statistical Methodology)*, 67(1):91–108, 2005.

Ryan J Tibshirani. Adaptive piecewise polynomial estimation via trend filtering. 2014.

Nikolaus Umlauf and Thomas Kneib. A primer on bayesian distributional regression. *Statistical Modelling*, 18(3-4):219–247, 2018.

Martin J Wainwright. *High-dimensional statistics: A non-asymptotic viewpoint*, volume 48. Cambridge university press, 2019.

Yu-Xiang Wang, James Sharpnack, Alexander J Smola, and Ryan J Tibshirani. Trend filtering on graphs. *Journal of Machine Learning Research*, 17(105):1–41, 2016.

Steven Siwei Ye and Oscar Hernan Madrid Padilla. Non-parametric quantile regression via the k-nn fused lasso. *Journal of Machine Learning Research*, 22(111):1–38, 2021.

Zhi Zhang, Carlos Misael Madrid Padilla, Xiaokai Luo, Oscar Hernan Madrid Padilla, and Daren Wang. Dense relu neural networks for temporal-spatial model. *arXiv preprint arXiv:2411.09961*, 2024.